

# **FORMULATION AND EVALUATION OF NANOPARTICLES OF HMG -CoA REDUCTASE INHIBITOR**

A Synopsis of the Ph.D. Thesis

Submitted to

**Gujarat Technological University, Ahmedabad**

By

**Ramani Vinodkumar Devchandbhai**

Enrollment No. 129990990011

Branch: Pharmacy

Under supervision of

**SUPERVISOR**

Prof. Dr. G. K. Jani  
SSR College of Pharmacy  
Sillvassa, India.

**CO- SUPERVISOR**

Dr. Vijaykumar B. Sutariya,  
USF College of Pharmacy  
University of South Florida  
MDC 30, USA.



**GUJARAT TECHNOLOGICAL UNIVERSITY, AHMEDABAD**

November - 2020

---

## Index

1	Title of the thesis and abstract .....	3
2	Brief description on the state of the art of the research topic .....	4
3	Definition of the Problem .....	5
4	Objective and Scope of work .....	6
5	Original contribution by the thesis.....	6
6	Methodology of Research, Results .....	7
7	Achievements with respect to objectives .....	31
8	Conclusion .....	32
9	List of publications and Presentations .....	33
10	References.....	34

---

## 1 TITLE OF THE THESIS AND ABSTRACT

### 1.1 Title of the thesis

Formulation and evaluation of nanoparticles of HMG-CoA reductase inhibitor

### 1.2 Abstract

#### **Objective:**

The HMG-CoA reductase inhibitors are the most extensively used to lower blood cholesterol for the prevention of cardiovascular disease. Pitavastatin calcium (PTV) is a relatively newly developed, potent, non-purine, synthetic HMG-CoA reductase inhibitor which has greater efficacy in reducing the low-density lipoprotein-cholesterol (LDL-C) and change in other lipoprotein compared to other statins. However, its poor water solubility restricts its clinical effectiveness. The nanoparticle is one of the promising approaches to enhance solubility and dissolution performance, and thereby bioavailability of the poorly soluble drug. Hence, the present study was undertaken to prepare PTV nanoparticles using the design of experiment approach.

#### **Method:**

The PTV nanoparticle was developed by the emulsion solvent evaporation technique followed by freeze-drying. Initially, various process and formulation variables were evaluated and screened using the Plackett-Burman design in which 7 factors at 2 levels were tested at 12 runs. Thereafter, a response surface optimization approach, Box-Behnken Design, was used to study the effects of critical variables on desired attributes. Spectroscopic and thermal evaluation of optimized nanoparticle were performed. The optimized nanoparticles were incorporated into the tablet and assessed for *in-vitro* dissolution and *in-vivo* pharmacokinetic behavior.

#### **Results:**

Statistical analysis of Plackett-Burman design revealed that stabilizer concentration, injection flow rate, and stirring rate were the most influential factors affecting the nanoparticle characteristics. The average particle size, polydispersity index, and zeta potential of nanoparticles optimized using Box-Behnken design were 207.8 nm, 0.141, and -20.71 mV respectively. The scanning electron microscopy (SEM), x-ray diffraction (XRD), and differential scanning calorimetry (DSC) study demonstrated that there was a reduction in crystallinity during the processing and confirm to the amorphization of the drug in its nano-form. Additionally, optimized PTV nanoparticles showed a significant improvement in solubility of prepared nanoparticles by 58.95-fold

---

in distilled water and 32.01-fold in PBS pH 6.8. Further, this result also supported the dissolution profile of nanoparticle loaded tablets which shows significant high dissolution efficacy and low mean dissolution time compared to the conventional product. In-vivo pharmacokinetic study of PTV nanoparticle-loaded tablets indicated a 1.76-fold improvement in oral bioavailability compared to the marketed tablet. Finally, the optimized nanoparticles as well as nanoparticles loaded tablets were found to be stable over three months.

### **Conclusion:**

It was concluded that the experimental design approach, PBD followed by BBD has been successfully implemented to screen the variables and optimize the PTV nanoparticles. The nanotechnology strategy was found to be a viable approach to enhance the solubility of drug which leads to improvement in *in-vitro* dissolution performance and *in-vivo* bioavailability of PTV. From the above studies, it is evident that developed novel conventional oral formulation of PTV can effectively be used in the treatment of hypercholesterolemia for better efficacy and clinical outcome.

## **2 BRIEF DESCRIPTION ON THE STATE OF THE ART OF THE RESEARCH TOPIC**

The formulation of poorly water soluble drugs is a big challenge for the pharmaceutical industry. It has been reported that about 70% of new drug candidates have been shown to have poor aqueous solubility. In the present study, a relatively newly developed, potent, non-purine, synthetic HMG-CoA reductase inhibitor, Pitavastatin calcium (PTV) was used to improve its poor solubility and dissolution rate.

A nanotechnology is an effective approach that can increase the dissolution rate of poorly water-soluble drugs by raising their saturation solubility, thus improving drug bioavailability. This approach generally produces dispersions of drug nanoparticles in a liquid medium (typically water), which are called ‘nanosuspensions’. To develop nanosuspension, the emulsion solvent evaporation technique has been reported as a relatively simple and easy to scale up process. The major downside of such a bottom-up technique is to maintain the nano size of particles. This problem can be overcome by the incorporation of suitable stabilizers and by freeze-drying. Further, to minimize the trial runs, the design of experiment approach, PBD followed by BBD has been implemented to screen the variables and optimize the PTV nanoparticles. Additionally,

---

the prepared nanoparticles were transformed into a tablet dosage form to ease the application of the drug.

### **3 DEFINITION OF THE PROBLEM**

Pitavastatin calcium (PTV) is a relatively newly developed, potent, non-purine, synthetic HMG-CoA reductase inhibitor.<sup>[1]</sup> This new statin is safe and well-tolerated in the treatment of patients with hypercholesterolemia.<sup>[2]</sup> The potency of PTV is dose-dependent and the absolute bioavailability of is 51%.<sup>[3]</sup> PTV is a class II drug as it has aqueous solubility (reported 0.000657 mg/mL)<sup>[4, 5]</sup> and high permeability (log P is 4.82).<sup>[6]</sup> This is due to several factors such as low solubility in water, transmembrane efflux via P-glycoprotein.<sup>[7]</sup>

One of the approaches to enhance the oral bioavailability of P-glycoprotein (P-gp) substrate drugs is to co-administered with P-gp inhibitors such as cyclosporine-A (CsA).<sup>[8]</sup> However, the use of cyclosporine-A is discouraged due to its immunosuppressant side effect. Thus instead of using therapeutic agents, it is advisable to use some excipients which having proven Pgp inhibitor activity such as pluronic P85, vitamin E-TPGS, PEGs, tween 80, cremophor EL, sodium caprate, and dimethyl- $\beta$ -cyclodextrin.<sup>[9]</sup> However, the high concentration of P-gp inhibitors is not advisable for oral consumption which may lead to changes in absorption, distribution, and elimination kinetics of toxins.<sup>[10]</sup> Submicron size particle of drug stabilized by a minimum amount of P-gp inhibitor may serve the purpose to minimize toxicity generated by P-gp inhibitors.

Besides, several studies have already been carried out to overcome the PTV limitation of aqueous solubility and dissolution rate, such as the preparation of solid dispersions,<sup>[11]</sup> co-crystal,<sup>[12]</sup> inclusion complexes,<sup>[13]</sup> self-microemulsifying drug delivery system (SMEDDS),<sup>[14]</sup> etc. However, the major problem of these formulations like poor loading, biocompatibility, biodegradability of excipients, and scale-up difficulty limits the clinical translation of drugs. Compared to other approaches reduction of particle size to the sub-micron range is a promising formulation strategy to enhance the dissolution rate, the saturation solubility and so to enhance the oral bioavailability of poorly soluble drugs.<sup>[15]</sup> Thus in this study attempt will be made to the development of Pitavastatin nanoparticle using a P-gp inhibitor as a stabilizing agent.

---

## 4 OBJECTIVE AND SCOPE OF WORK

### 4.1 Objective

- Development and evaluation of Pitavastatin nanoparticle using Design of experiment approach.
- Enhance solubility and dissolution rate of poorly soluble drug (Pitavastatin calcium).
- To study *in-vivo* pharmacokinetic behavior of formulation containing developed Pitavastatin nanoparticle.

### 4.2 Scope of work

Cardiovascular disease remains the leading cause of death in the geriatric population which can be controlled by treating the major risk factors. Statins are the most extensively used drug to lower blood cholesterol for the prevention of cardiovascular disease. However, its poor water solubility restricts its clinical effectiveness demands an urgent need for a novel formulation strategy which can enhance solubility and dissolution performance and thereby bioavailability. After clinical trials and fulfillment of other regulatory requirements, the developed nanoparticle loaded tablet formulation may prove to be a boon to society at large for the complete treatment of hypercholesterolemia.

## 5 ORIGINAL CONTRIBUTION BY THE THESIS

- The developed HPLC method with an optimized mobile phase is validated, less time-consuming, and user friendly for the quantification of PTV in bulk and tablet samples.
- The bottom-up technology used in this work provides a simple and robust platform for the bottom-up generation of nanoparticles. Further investigations on this technology such as the role of process and formulation variables using the experimental design approach provide an efficient means to optimize the nanoparticles and scale-up.
- The nanotechnology strategy was found to be a viable approach to enhance the solubility of drug which leads to improvement in *in-vitro* dissolution performance and *in-vivo* bioavailability of PTV. It can be a promising novel conventional oral formulation in the treatment of hypercholesterolemia with better efficacy and clinical outcome.

---

## 6 METHODOLOGY OF RESEARCH, RESULTS

### 6.1 Preformulation studies

#### 6.1.1 Identification and purity of the pure drug

The drug sample was subjected to visual and sensory inspection to check color, odor, and appearance to confirm the identity of the drug sample. It was observed that the sample was off white, odorless, and crystalline. The results comply with the standard as per Indian pharmacopoeia 2018<sup>[16]</sup> which confirms the identity of the drug sample. Melting point is one of the identification and purity test for organic substances. Hence, it was determined for the sample by the capillary method using melting point apparatus. It was observed that the melting point of sample was  $192 \pm 0.5$  °C. The results comply with standard value ( $190^{\circ}\text{C}$ - $192^{\circ}\text{C}$ ),<sup>[17]</sup> which confirms the identity of the drug sample. The  $\lambda_{\text{max}}$  was determined by scanning the standard solution of PTV (10 µg/ml) through the UV range (200 to 400 nm) against blank and compared with the standard value. UV spectrum of PTV in methanol, distilled water, and phosphate buffer pH 6.8 showed maximum absorbance ( $\lambda_{\text{max}}$ ) at 245 nm which further complies with the identity and purity of the drug sample.<sup>[16]</sup>

The assay of pure drug was determined using in-house developed HPLC method ( $Y = 0.085X - 0.0023$ ;  $R^2 = 0.9997$ ).<sup>[18]</sup> The assay of PTV pure drug was found to be  $99.40 \pm 0.044$  %, which complies with the standard limit of 98% to 102% as per Indian pharmacopoeia 2018.<sup>[16]</sup>

#### 6.1.2 Drug- excipients compatibility

The IR spectroscopy was conducted using an FTIR spectrophotometer and the spectrum was recorded in the wavelength region of  $4000 - 400 \text{ cm}^{-1}$ . IR spectroscopy study of pure drug and physical mixtures with excipients were conducted using an FTIR spectrophotometer analyzer to detect the existence of a possible interaction between drug and excipients. The obtained FT-IR spectrum graph of pure drug compiles with standard data (**Table 1**) which further confirms the identity and purity of the drug. Moreover, the characteristic peaks of the drug appear in the spectra of the physical mixture of drug and excipients (**Table 1**) were near to standard frequency of functional groups<sup>[19]</sup> which indicates no interaction between the drug and the excipients.

**Table 1. FTIR analysis for pure drug and physical mixture of PTV with excipients**

Functional group	Standard Frequency (cm <sup>-1</sup> ) <sup>[19]</sup>	Observed Frequency (cm <sup>-1</sup> )	
		Pure Drug	Physical Mixture
O- H Stretching	3650-3200	3315	3356
Aromatic C-H stretching	3000-2853	2893	2883
O=C=O Stretching	2349	2345	2345
O-H bending	1440-1395	1433	1591
C-F stretching	1400-1000	1076	1427
C-N stretching	1250-1020	1219	1219

### 6.1.3 Analytical method development

#### 6.1.3.1 HPLC method

In this work, we demonstrate the use of simplex centroid design with axial points in a pseudo component representation for determining the optimal mobile phase composition that results in an improved peak quality of pitavastatin calcium in bulk and tablet formulation using RP-HPLC. The optimization of the HPLC method involves several variables whose influence has been widely studied. However, in most of the cases, only process variables are taken into account.<sup>[20-22]</sup> Therefore, the influence of mixture composition on peak quality parameters of Pitavastatin calcium in bulk and tablet dosage form has been studied using a simplex mixture design.

A simplex centroid design with axial points in a pseudo-component representation (**Figure 1**) was generated from the pure mixture components.<sup>[23-26]</sup> Twelve ternary mixture mobile phases corresponding to augmented design points were tested to separate the drug in the sample (**Table 2**). The statistical analysis was performed to generate the polynomial equation for each response. The results of the experimental design were statistically tested for full and in portion to get best-fitted model which accurately describes changes in the proportion of these solvents in the mobile phase close to the region of the optimal peak quality. The desirability approach was used to determine the optimal mobile phase composition.

The method (**Table 3**) demonstrated optimum chromatographic separation (**Figure 2**) with isocratic elution of the mobile phase containing a mixture of acetonitrile-water (pH 3.0)-tetrahydrofuran (43:55:02, v/v/v) with a flow rate at 1.0 ml/minute. Furthermore, the method was validated as per the ICH Q2 (R1) guidelines<sup>[27]</sup> using specificity, linearity, accuracy, precision, sensitivity, system suitability, and robustness (**Table 4**). The optimization strategy using the experimental design approach is a powerful tool to acquire the maximum quality data while performing a minimum



number of experiments. The mobile phase composition was successfully optimized using a simplex centroid mixture design with a desirability approach. Additionally, the developed method can be applied for routine quantitative analysis of pitavastatin calcium in bulk and tablet dosage form as it was found to be simple, sensitive, and robust.

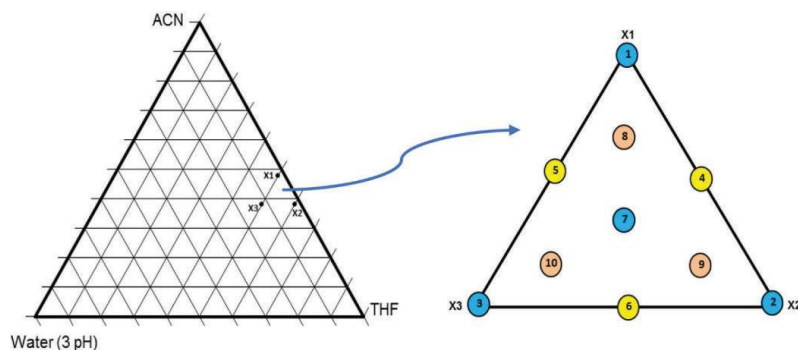


**Figure 1. Simplex centroid design with axial points in a pseudo component**

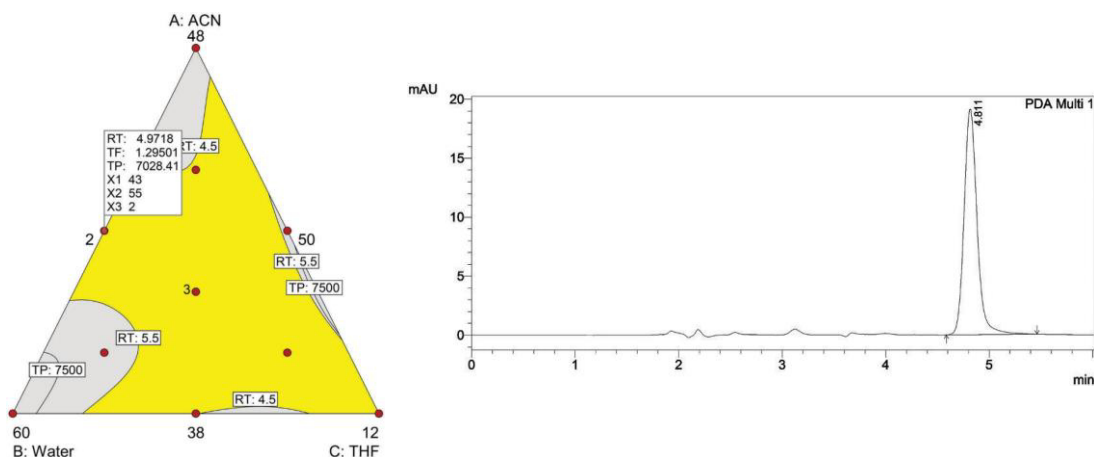


**Figure 2. Overlaid contour plot for RT ( $Y_1$ ), TF ( $Y_2$ ), and TP ( $Y_3$ ) and validated experimental chromatogram**

**Table 2. Mobile phase compositions of mixture design and respective responses**

Run	Composition of pseudo-components			% Composition	Responses			Space type
	$X_1$	$X_2$	$X_3$	ACN: Water: THF	$Y_1$ : RT	$Y_2$ : TF	$Y_3$ : TP	
1	1	0	0	48:50:2	4.13	1.236	6129	V
2	0	1	0	38:60:2	6.60	1.227	7699	V
3	0	0	1	38:50:12	4.97	1.205	7182	V
4	0.5	0.5	0	43:55:2	4.99	1.287	7026	CE
5	0.5	0	0.5	38:55:7	5.64	1.188	7467	CE
6	0	0.5	0.5	43:50:7	4.52	1.22	6740	CE
7	0.333	0.333	0.333	41.33:53.33:5.34	5.10	1.242	7090	C
8	0.667	0.167	0.167	44.67:51.66:3.67	4.48	1.243	6755	ACB
9	0.1667	0.6667	0.1667	39.67:56.66:3.67	5.65	1.255	7408	ACB
10	0.167	0.167	0.667	39.67:51.66:8.67	4.98	1.203	7154	ACB
11	0.333	0.333	0.333	41.33:53.33:5.34	5.07	1.254	7230	C
12	0.333	0.333	0.333	41.33:53.33:5.34	5.07	1.24	7143	C

ACN indicates: Acetonitrile; THF, Tetra hydro furan; V, Vertex; CE, Centers of edges; C, Center; ACB, Axial check blends;  $Y_1$ , Retention time (RT);  $Y_2$ , Tailing Factor (TF);  $Y_3$ , Theoretical Plates (TP);  $X_1$ , (48:50:2);  $X_2$ , (38:60:2);  $X_3$ , (38:50:12)

**Table 3. Instrumentation and Chromatographic procedure**

Parameter	Value
System	Shimadzu UFLC Prominence (Kyoto, Japan)
Pump	LC-20AD, Binary
Detector	PD-M20A PDA
Software	LC solution
Column	C18 column (kromasil, 250×4.6 mm, 5 µm, 100 Å)
Mobile phase	43:55:2 v/v/v (ACN:H <sub>2</sub> O:THF)
pH	3 (adjusted using 0.1% TFA)
Flow rate	1mL/min
Injection volume	20 µL
Concentration of solution	1 µg/mL
Detection wavelength	249 nm

**Table 4. Summary of validation parameters for the proposed HPLC method.**

Parameters	Results	Inference
<b>Linearity</b>		
Linearity range (ng/mL)	10-500	Method was linear
Correlation coefficient ( <i>r</i> <sup>2</sup> )	0.9993	
Regression equation	y = 166.54x + 742.43	
<b>Sensitivity</b>		
LOD (ng/mL)	1.949	Method was sensitive
LOQ (ng/mL)	5.907	
<b>Precision (% RSD)</b>		
<b>Repeatability</b>	<b>Mean ± SD</b>	<b>% RSD</b>
50	8980.83 ± 80.23	0.893
100	17713.6 ± 199.21	1.125
250	41110.5 ± 689.16	1.676
<b>Intraday</b>		
50	8989 ± 75.44	0.839
100	17726.07 ± 178.37	1.006
250	41139 ± 631.17	1.534
<b>Inter day</b>		
50	8972.67 ± 78.92	0.88
100	17686.96 ± 217.91	1.232
250	41032.11 ± 576.31	1.405
<b>Accuracy</b>		
80	98.97 ± 0.83	0.841
100	100.14 ± 0.96	0.963
120	100.48 ± 0.32	0.314
<b>Robustness (% RSD)</b>	Flow Rate, pH, Extraction time, Mobile phase Ratio	< 2.0
		Method was robust

n=6 for SD

**6.1.3.2 UV Spectroscopic method**

UV Spectroscopic method for quantification of PTV in samples was developed in different solvent systems at appropriate absorbance maxima as described in **Table 5**. Regression equations and their correlation coefficients ( $r^2$ ) are presented in **Table 5**.

**Table 5. Results of regression analysis for UV calibration data for Pitavastatin calcium**

Solvent	Co-solvent	Range (µg/ml)	Absorbance maxima ( $\lambda_{max}$ )	Regression equation	Regression coefficient ( $R^2$ )
Methanol	-	2 – 10	245	$y = 0.0851x - 0.0023$	0.9997
Distilled water	Methanol	2 – 10	245	$y = 0.0701x - 0.0074$	0.9986
0.1N HCL	Methanol	1 – 10	250	$y = 0.0778x - 0.0207$	0.9988
PBS pH 6.8	Methanol	2 – 12	245	$y = 0.0788x - 0.02$	0.9992
Acetone	-	1 – 10	331	$y = 0.0778x - 0.0207$	0.9857

## 6.2 Development of PTV Nanoparticle formulation

### 6.2.1 Method of preparation of PTV nanoparticles

The PTV nanoparticle suspension was prepared using the emulsion solvent evaporation technique (**Figure 3**). In this method, the organic phase was prepared by dissolving drug in organic solvent. The aqueous phase was prepared by dissolving stabilizing agent in deionized water. The aqueous phase was stirred in a 250 mL beaker at a specific stirring rate and temperature using a magnetic stirrer equipped with hot plate (RCT Basic, IKA India Pvt. Ltd., Bengaluru). Then, the organic phase was poured at a precise rate in the aqueous phase using syringe pump (Infusa 101P, Devay Medical Technologies, Vadodara). The obtained suspension was continuously stirred at the same temperature until complete evaporation of the organic phase. Finally, nanosuspension was immediately placed at -80 °C (Deep Freezer, SU105UE, Undercounter, Stirling Ultracold, USA) for 12 hr and freeze-dried (MSW- 137, Macro scientific works, Delhi) at -40 °C for 48 h. The obtained nanoparticles were kept in a desiccator at 4 °C until further analysis.

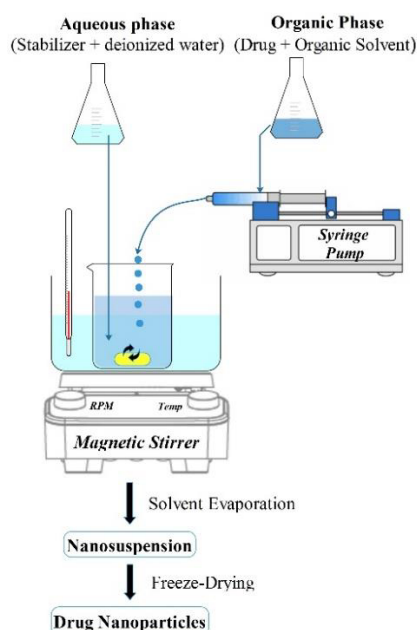


**Figure 3. Process flowchart for nanoparticle development**

## 6.2.2 Screening of variables using Plackett-Burman design

### 6.2.2.1 Selection of variables

The prior scientific study was reviewed to identify the formulation and process variables for the current preparation method. The average particle size and polydispersity index (PDI) were considered as critical properties of nanoparticle since these properties are expected to influence its clinical efficacy. Seven formulation and process variables that affect the properties of nanoparticle were specified and included in the screening study **Table 6**.

**Table 6. Selection of independent variables**

Sr. No.	Independent Variables	Range	Reason for selection
<b>Formulation variables</b>			
1	Organic Phase type	Acetone and Methanol	A selected solvent should be able to dissolve the drug and miscible with an aqueous phase over the concentration range. Changing the solvent, not only alters the supersaturation conditions, but also affects viscosity and surface tension, and consequently changes the nucleation rate. <sup>[28]</sup>
2	Organic Phase volume	6 – 12 mL	The organic phase volume alters the drug concentration which could affect the particle characteristics.
3	Stabilizer type	Pluronic P85 and TPGS - 1000	It stabilizes the formed nanoparticle and stops further growth and aggregation by the free energy reduction, steric hindrance, and electrostatic stabilization. <sup>[29]</sup> Additionally, selected stabilizers have some permeation enhancing effect through P-gp inhibition. <sup>[30]</sup>
4	Stabilizer concentration	0.01-0.04 % w/v	A low concentration of stabilizer may not sufficient and promotes discreet coating of nanoparticle while higher concentration may promote aggregation through depletion flocculation mechanism. <sup>[31]</sup>
<b>Process variables</b>			
5	Stirring speed	500-2500 RPM	The mechanical stirring helps to promote even degree of supersaturation and also intensifies micro-mixing which increases the rate of diffusions and mass transfer between multiphase system. This favors the generation of small particles due to rapid and uniform nucleation. <sup>[32]</sup>
6	Temperature of aqueous phase	30-65 °C	The temperature affects the equilibrium saturation, supersaturation concentration, diffusion rate, and viscosity of the system. Additionally, the change in the temperature during nucleation also affects the physical property of nanoparticle. <sup>[32, 33]</sup>
7	Injection Flow rate (rate of organic phase addition)	0.5-1.5 mL/min	The Injection flow rate affects the extent of mixing per unit time which strongly influences the particle size distribution. <sup>[34]</sup> Furthermore, It also alters the degree of supersaturation and therefore strongly influences the nucleation rate and particle growth kinetics. <sup>[28]</sup>
<b>Variables kept constant</b>			
8	Drug quantity	100 mg	The drug quantity was kept constant (100 mg) for all batches of nanosuspension So that comparative observation can be drawn for each independent factor.
9	Final volume of Nanosuspension (aqueous phase + organic phase)	50 mL	In this study, the final volume of nanosuspension was kept constant (50 mL) and the volume of organic phase was varied thus the volume of an aqueous phase and its ratio to the organic phase gets varied by default. it allows us to an indirect estimation of the effect of ratio (organic phase to aqueous phase) on the physical properties of nanoparticles.

---

#### 6.2.2.2 Plackett-Burman design setup and analysis

Plackett-Burman (PB) designs are very efficient screening designs when only the main effects are of interest. With the help of this design, the construction of very economical designs with the run number a multiple of four (rather than a power of 2).<sup>[35]</sup> PB designs are used for screening experiments because, in a PB design, the main effects are, in general, heavily confounded with two-factor interactions.

In the present study, we have used the Plackett-Burman design (PBD) for the screening of variables for the development of PTV nanoparticle. Seven factors at two levels were tested at 12 runs to study the effect of formulation and process variables on particle size and PDI (**Table 7**). High and low levels of factors were decided according to previous study and review of data. *Design expert*<sup>®</sup> software (V-10.0.1.0, State-Ease Inc., Minneapolis, MN, USA) was used to generate and randomize the design matrix which is then statistically analyzed. The factor coefficients and significance of the model were evaluated through multiple regression analysis and ANOVA.

Based on PB design analysis (**Figure 4** and **Table 8**), the stabilizer concentration, stirring rate, and injection flow rate were the most critical factors which affect the particle size and polydispersity index of nanoparticle formulation. Additionally, less influential factors like stabilizer type (TPGS-1000), organic phase type (acetone), organic phase volume (12 mL), organic phase type (acetone), organic phase volume (12 mL), and temperature (65 °C) were set at a favorable level. The subsequent experimentation was performed using these critical parameters to understand and analyze the nature of interactions among them using response surface methods.

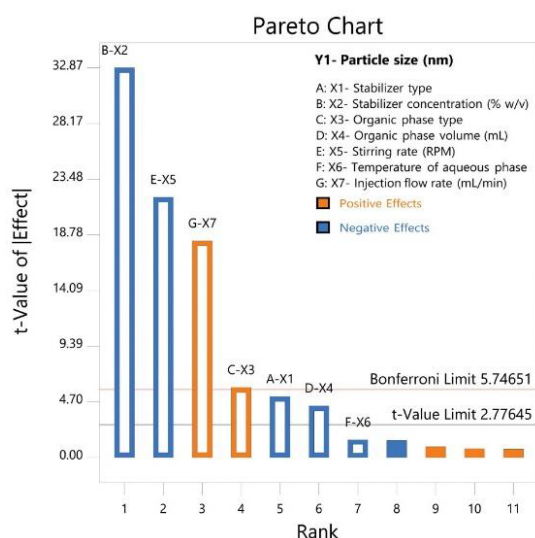
- ❖ Based on screening design following factors kept constant:
  - Stabilizer type: TPGS 1000
  - Organic phase type: Acetone
  - Organic phase volume: 12 mL
  - Temp. of aqueous phase: 65 °C
- ❖ Based on screening design following factors needs to be further optimization:
  - Stabilizer concentration (% w/v):  $0.04 \pm 0.02$  (0.2 to 0.06)
  - Injection flow rate (mL/min):  $0.5 \pm 0.3$  (0.2 to 0.8)
  - RPM:  $2500 \pm 1000$  (1500 to 3500)

**Table 7. Plackett-Burman screening design output matrix with results**

Batch Code	Independent variables							Dependent variables	
	Stabilizer type	Stabilizer con. (% w/v)	Org. Phase Type	Org. Phase Vol. (mL)	Stirring rate (RPM)	Temp. of Aqu. Phase (°C)	Inj. Flow Rate (mL/min)	PS (nm)	PDI
	$X_1$	$X_2$	$X_3$	$X_4$	$X_5$	$X_6$	$X_7$	$Y_1$	$Y_2$
PNS1	TPGS-1000	0.01	MeOH	12	500	65	1.5	743.4	0.453
PNS2	Pluronic P85	0.01	MeOH	6	2500	65	0.5	503.2	0.443
PNS3	Pluronic P85	0.04	MeOH	6	2500	65	1.5	390.9	0.402
PNS4	Pluronic P85	0.04	MeOH	12	500	30	0.5	390.8	0.354
PNS5	Pluronic P85	0.04	ACE	12	2500	30	1.5	305.3	0.319
PNS6	TPGS-1000	0.04	ACE	6	500	65	0.5	324.3	0.226
PNS7	TPGS-1000	0.01	ACE	6	2500	30	1.5	576.4	0.439
PNS8	Pluronic P85	0.01	ACE	12	500	65	1.5	768.5	0.55
PNS9	TPGS-1000	0.01	MeOH	12	2500	30	0.5	450.7	0.305
PNS10	TPGS-1000	0.04	ACE	12	2500	65	0.5	113.1	0.068
PNS11	Pluronic P85	0.01	ACE	6	500	30	0.5	647.2	0.508
PNS12	TPGS -1000	0.04	MeOH	6	500	30	1.5	545.6	0.435

PS indicates: particle size; PDI, polydispersity Index; PNS, Pitavastatin nanoparticle screening batch; TPGS-1000, D- $\alpha$ -Tocopherol polyethylene glycol 1000 succinate; MeOH, Methanol; ACE, Acetone; RPM, revolution per minute

**A**



**B**

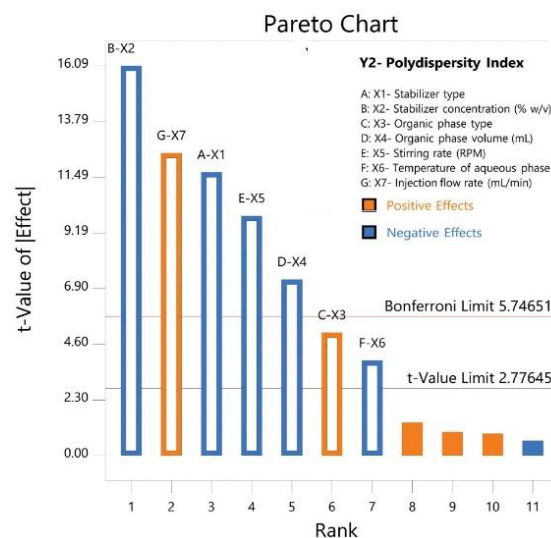


**Figure 4. Pareto chart for A) Particle size ( $Y_1$ ) and B) Polydispersity index ( $Y_2$ )**

**Table 8. Regression analysis for dependent variables**

Independent variables	Particle size ( $Y_1$ )			Polydispersity index ( $Y_2$ )		
	Coefficient	P-Value	% Contribution	Coefficient	P-Value	% Contribution
Intercept	480.03	< 0.0001	-	0.3752	0.0002	-
$X_1$ - Stabilizer type	-21.12	0.0068	1.33	-0.0542	0.0003	<b>18.30</b>
$X_2$ - Stabilizer con.	-134.87	< 0.0001	<b>54.47</b>	-0.0745	< 0.0001	<b>34.62</b>
$X_3$ - Org. phase type	24.23	0.0041	1.75	0.0235	0.0071	3.44
$X_4$ - Org. phase vol.	-17.9	0.0120	0.95	-0.0337	0.0019	7.07
$X_5$ - Stirring rate	-90.1	< 0.0001	<b>24.31</b>	-0.0458	0.0006	<b>13.10</b>
$X_6$ - Temp. of aq. phase	-6.13	0.2093	0.11	-0.0182	0.0172	2.05
$X_7$ - Inj. flow rate	74.98	< 0.0001	<b>16.83</b>	0.0578	0.0002	<b>20.86</b>

## 6.2.3 Optimization of nanoparticle formulation using Box-Behnken design

### 6.2.3.1 Box-Behnken design setup

A response surface method, the Box-Behnken design (BBD) was applied to optimize PTV nanoparticle formulation. *Design expert® 11.0.4.0* software (State-Ease Inc., Minneapolis, MN, USA) was used for statistical analysis and optimization. The independent variables were  $X_1$ : stabilizer concentration,  $X_2$ : injection flow rate, and  $X_3$ : stirring rate, while  $Y_1$ : particle size,  $Y_2$ : polydispersity index,  $Y_3$ : zeta potential were selected as dependent variables. As per the design total of 14 batches (12 design points and 2 additional center points to evaluate the lack of fit) were prepared by varying the factor levels (**Table 9**).

**Table 9. Box-Behnken design setup and results**

Batch	Independent factors			Dependent factors		
	Stabilizer concentration (% w/v)	Injection flow rate (mL/min)	stirring rate (RPM)	PS (nm)	PDI	ZP (mV)
	$X_1$	$X_2$	$X_3$	$Y_1$	$Y_2$	$Y_3$
PNO1	0.04	0.8	1500	485.2	0.512	-14.7
PNO2	0.04	0.5	2500	309.1	0.181	-17.0
PNO3	0.06	0.8	2500	736.4	0.493	-14.2
PNO4	0.02	0.2	2500	104.2	0.191	-21.9
PNO5	0.02	0.5	3500	199.4	0.165	-15.1
PNO6	0.06	0.2	2500	372.7	0.316	-18.2
PNO7	0.06	0.5	1500	688.5	0.418	-12.1
PNO8	0.02	0.5	1500	245.4	0.211	-16.8
PNO9	0.06	0.5	3500	572.3	0.341	-9.9
PNO10	0.04	0.2	1500	188.2	0.392	-17.7
PNO11	0.04	0.8	3500	456.8	0.433	-12.8
PNO12	0.04	0.2	3500	149.4	0.382	-15.9
PNO13	0.04	0.5	2500	328	0.187	-17.4
PNO14	0.02	0.8	2500	256.2	0.238	-19.2

RPM, revolution per minute; PS, particle size; PDI, polydispersity index; ZP, zeta potential. For all batches: The drug quantity was 100 mg, 12 mL of Acetone as organic phase, 38 mL of deionized water as an aqueous phase. The nanoparticles were prepared using the emulsion solvent evaporation technique followed by freeze-drying.

### 6.2.3.2 Box-Behnken design analysis

It was observed that in all cases there exists a reasonable impact of independent variables. A quadratic model consisting of main and interactive effects was used to estimate the response. The factor coefficients and significance of the model were evaluated through multiple regression analysis and ANOVA (**Table 10**). The model  $F$  ratios were statistically significant ( $p < 0.05$ ) with  $r^2$  value in the range of 0.9614 - 0.9982. For all responses, adjusted and predicted  $r^2$  values were in reasonable agreement, demonstrating the mathematical model describes the data adequately. However, certain model terms for all three responses having  $p > 0.05$  require a model



reduction to improve the more precise predictive ability of the model (**Table 10**). Removal of these insignificant terms improved the model for all three responses. The  $F$  statistics in portion was used to test the generated reduced model. The result shows that the  $F_{critical}$  at  $\alpha = 0.05$  ( $Y_1$ ,  $F_{critical} = 6.59$ ;  $Y_2$ ,  $F_{critical} = 6.94$ ;  $Y_3$ ,  $F_{critical} = 6.39$ ) is greater than  $F_{tabulated}$ , indicates that the term ( $b_{12}$ ,  $b_{13}$ ,  $b_{22}$ ,  $b_{33}$ ) for  $Y_1$ , ( $b_{13}$ ,  $b_{11}$ ) for  $Y_2$  and  $b_{12}$ ,  $b_{13}$ ,  $b_{23}$ ,  $b_{11}$ ) for  $Y_3$ , does not contribute significantly to the prediction of responses and therefore can be omitted from the full model (**Table 11**). However, to maintain the hierarchy of model  $b_{22}$  term  $Y_1$  was not omitted in the reduced model. Furthermore, the reduced model shows a lower  $p$ -value compared to the full model favors the reduced model for further optimization. Additionally, an insignificant lack of fit for all responses also implies that the models were adequate for the prediction with the range of experimental variables.

Direct interpretation of reduced polynomial equations may lead to errors since interaction and quadratic terms are also significant. Therefore, 2D contour and 3D surface plots were generated. A nonlinear relationship is visible in all contour and surface plots (**Figure 5**). It offers a rational understanding of the plausible interaction(s) among the variables and helps to identify the design space by generating an overlaid contour plot (**Figure 6**).

**Table 10. Regression Analysis for BBD Design**

Coefficient code	$Y_1$ : PS			$Y_2$ : PDI			$Y_3$ : ZP		
	FM		RM	FM		RM	FM		RM
	Coefficient	$p$ -value	Coefficient	Coefficient	$p$ -value	Coefficient	Coefficient	$p$ -value	Coefficient
$b_0$	318.55	0.0004	342.7	0.184	0.0001	0.176	-17.2	0.0001	-16.95
$b_1$	195.59	< 0.0001	195.59	0.095	< 0.0001	0.095	2.325	< 0.0001	2.325
$b_2$	140.01	0.0001	140.01	0.049	0.0003	0.049	1.6	0.0001	1.6
$b_3$	-28.68	0.0386	-28.68	-0.027	0.0027	-0.027	0.95	0.0006	0.95
$b_{12}$	52.93	0.0167	52.93	0.033	0.0046	0.033	0.325	0.0798 <sup>ns</sup>	-
$b_{13}$	-17.55	0.2593 <sup>ns</sup>	-	-0.008	0.2436 <sup>ns</sup>	-	0.125	0.4199 <sup>ns</sup>	-
$b_{23}$	2.6	0.8552 <sup>ns</sup>	-	-0.017	0.0384	-0.017	0.025	0.8662 <sup>ns</sup>	-
$b_{11}$	77.66	0.0065	71.63	-0.01	0.1813 <sup>ns</sup>	-	0.3125	0.1151 <sup>ns</sup>	-
$b_{22}$	-28.84	0.1258 <sup>ns</sup>	-34.88	0.136	< 0.0001	0.138	-1.4875	0.0007	-1.55
$b_{33}$	30.19	0.1134 <sup>ns</sup>	-	0.11	0.0001	0.112	3.4125	< 0.0001	3.35

PS, particle size; PDI, polydispersity index; ZP, zeta potential; FM, full model; RM, reduced model; ns, not significant ( $p > 0.05$ )

**Table 11. Model testing summary**

Model parameters	$Y_1$ : PS		$Y_2$ : PDI		$Y_3$ : ZP	
	FM	RM	FM	RM	FM	RM
$df$	8	6	8	7	8	5
$F$ -value	79.27	83.83	167.84	152.24	178.34	178.15
$p$ -value (model)	0.0004	< 0.0001	0.00009	< 0.0001	0.0001	< 0.0001
$r^2$	0.994	0.986	0.997	0.994	0.998	0.991
$p$ -value (Lack of Fit)	0.294		0.216		0.515	
$F_{calculated}$	1.95		2.23		2.59	
$F_{critical}$ ( $\alpha=0.05$ )	6.59		6.94		6.39	

PS, particle size; PDI, polydispersity index; ZP, zeta potential; FM, full model; RM, reduced model



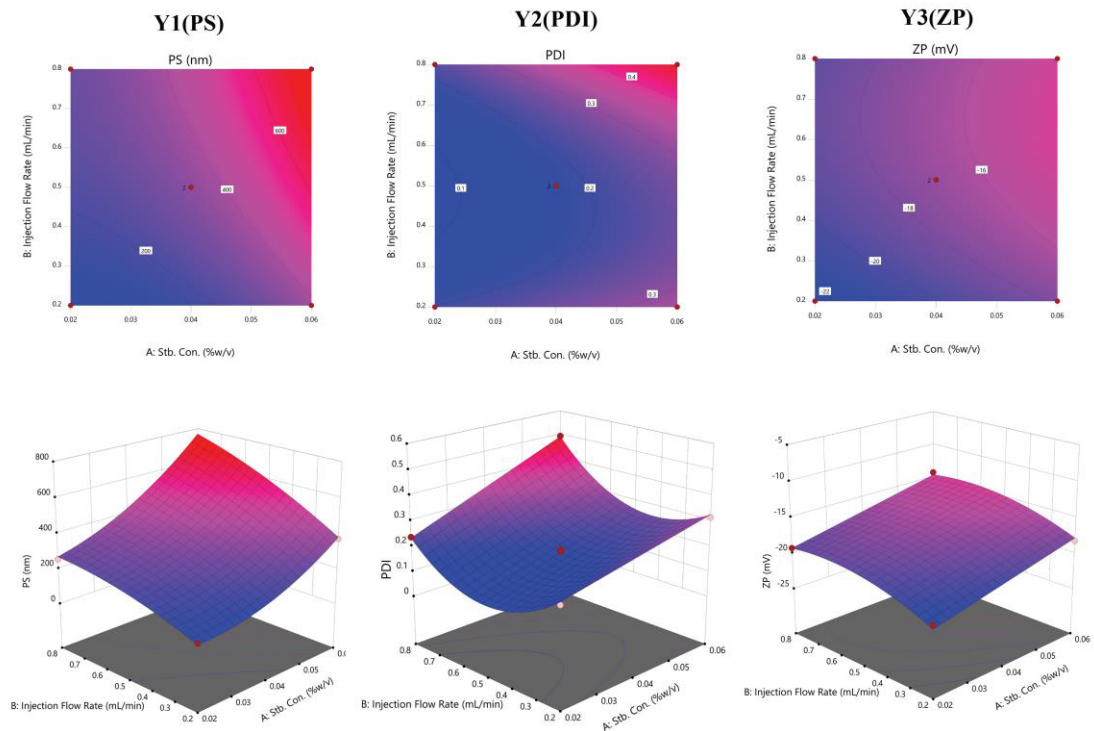


**Figure 5. Contour and 3D surface plots for Responses (For  $Y_1$ ,  $Y_2$ , and  $Y_3$ )**

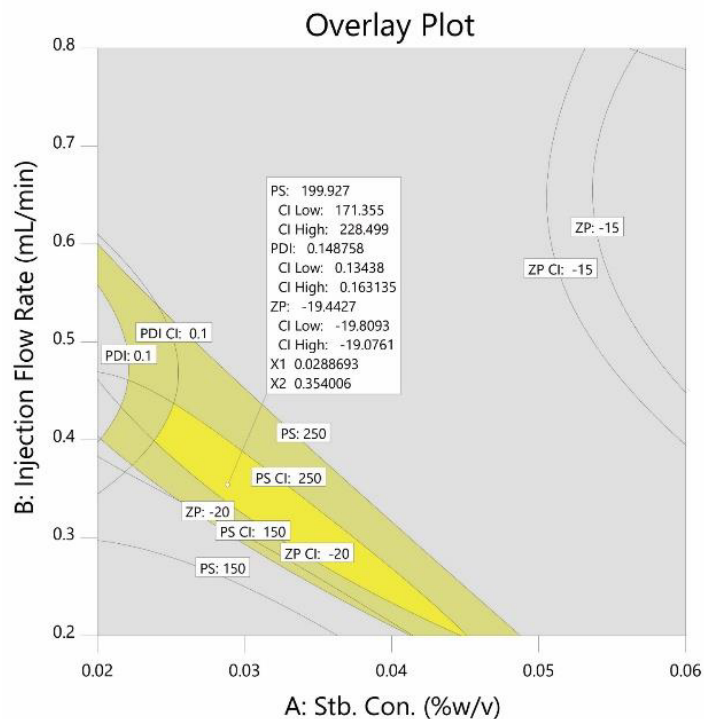


**Figure 6. Overlay contour plot with design space & optimized batch flag**

#### 6.2.3.2.1 Effect of stabilizer concentration

The stabilizer concentration shows a significant effect on PS ( $Y_1$ ) and PDI ( $Y_2$ ) ranging from 104.2 to 736.4 nm and 0.165 to 0.512 respectively. The positive coefficient of stabilizer concentration ( $X_1$ ) indicates that the PS and PDI of nanoparticles increase with  $X_1$  values increase. This could be attributed to the increase of drug solubility at

---

higher stabilizer concentration increase drug particle growth, further increasing the PS and PDI. Furthermore, interaction coefficient value ( $b_{12}$  and  $b_{13}$ ) indicates that variables like stirring rate and injection flow rate also contribute to PS and PDI of the nanoparticle. The zeta potential plays an important role in preventing aggregation and agglomeration; thus responsible for the long-term stability of nanoparticles.<sup>[36]</sup> **Table 9 and Figure 5** shows that the increase in the concentration of stabilizer induces a decrease in negative potential from -21.9 to -9.9 mV which may be attributed to steric stabilization by TPGS-1000.<sup>[37]</sup>

#### 6.2.3.2.2 *Effect of injection flow rate*

The addition rate of the organic phase to the aqueous phase has a substantial impact on the particle properties.<sup>[28]</sup> **Table 9** shows that an increase in injection flow rate from 0.2 to 0.8 mL/min causes an increase in PS, PDI, and ZP which was also illustrated in response surface plots (**Figure 5**). Such an effect can be explained by alteration in rate and degree of saturation strongly influence particle growth kinetics.<sup>[28]</sup> Additionally, the injection flow rate also affects the extent of mixing per unit time which alters the particle size distribution.<sup>[31, 34]</sup> Furthermore, interaction coefficient value ( $b_{12}$  and  $b_{23}$ ) indicates that variables like stabilizer concentration and stirring rate also contribute to PS and PDI of nanoparticle while ZP does not show any substantial difference indicates the absence of interactive impact on responses.

#### 6.2.3.2.3 *Effect of stirring rate*

There was a significant effect on PS, PDI, and ZP with a change in the stirring rate from 1500 to 3500 RPM. Particle size decreased with an increase in stirring rate (**Table 9**) this may be due to high micromixing increases the rate of diffusion and mass transfer between the multiphase and thus high homogenous supersaturation in a short time which causes rapid nucleation and generation of smaller particles. Simultaneously, the value of PDI also decreases with a high stirring rate due to uniform supersaturation. Hence, a higher stirring rate may favor the formation of smaller and more uniform drug particles.<sup>[32]</sup> However, in a certain situation at a high stirring rate there was an increase in PDI this can be explained by the high concentration of stabilizer triggers uneven particle growth indicates the presence of interaction. Additionally, the increases in the stirring rate induce an increase in the negative potential of nanoparticles which may prevent aggregation and particle growth of nanoparticles (**Table 9 and Figure 5**).

### 6.2.3.3 Checkpoint analysis and optimization

The optimization process was performed to develop the nanoparticle with desired characteristics by setting the response  $Y_1$  at 200 nm,  $Y_2$ , and  $Y_3$  at a minimum while independent variables were kept in the experimental range. Based on the set target, the software suggested various composition of formulation starting with the highest desirability value. The value of the desirability factor nearer to 1 indicated the optimum formulation. Additionally, an overlay plot was also constructed for graphical optimization (**Figure 9**). The yellow region in the plot represents the design space. However, to eliminate the uncertainty of experimental error, tolerance was set at 0.99 with a 95% confidence interval to improve the design space.<sup>[38]</sup>

The checkpoint analysis was done to validate the design and polynomial equation. For that, two batches PNOB1 (PTV nanoparticle optimized batch-1) and PNOB2 (PTV nanoparticle optimized batch-2) were selected from design space based on desirability and prepared to evaluate the responses. A low value of prediction error (< 10%) depicted that there was a reasonable agreement in predicted and experimental values (**Table 12**). However, the PNOB1 was selected as the final optimized batch due to its least prediction error. These results suggest the success of experimental design along with the desirability approach for the evaluation and optimization of the formulation.

**Table 12. Comparison of predicted and experimental values of responses**

Batch code	Factor value	Desirability	Predicted value			Experimental value*		
			PS (nm)	PDI	ZP (mV)	PS (nm)	PDI	ZP (mV)
PNOB1	$X_1=0.029$ , $X_2=0.354$ , $X_3=2291.4$	0.934	200	0.149	-19.44	$207.8 \pm 3.72$	$0.141 \pm 0.03$	$-20.71 \pm 0.47$
PNOB2	$X_1=0.031$ , $X_2=0.335$ , $X_3=2273.6$	0.939	200	0.164	-19.41	$189.1 \pm 4.32$	$0.179 \pm 0.05$	$-18.21 \pm 0.61$

\*All values are mean  $\pm$  SD (n = 3).  $X_1$ , stabilizer concentration (%w/v);  $X_2$ , injection flow rate (mL/min);  $X_3$ , stirring rate (RPM); PS, particle size; PDI, polydispersity index; ZP, zeta potential

## 6.2.4 Characterization of optimized PTV nanoparticle

### 6.2.4.1 Particle size, polydispersity index, and zeta potential

The particle size, polydispersity index, and zeta potential of the prepared formulations were determined by a dynamic light scattering technique using Zetatracc (Microtrac Inc., USA). The analysis was carried out using deionized water as disperse media at  $25 \pm 1$  °C.<sup>[39, 40]</sup>

The histograms of the particle size distribution for the final optimized batch (PNOB1) and unprocessed drug in terms of percent passing is presented in **Figure 7**. The mean

particle size of the unprocessed drug was  $5122.3 \pm 122.32$  nm, whereas  $207.8 \pm 3.72$  nm for optimized PTV nanoparticles. It shows ~246 times reduction in particle size in the case of PTV nanoparticles compared to that of the unprocessed drug. Many researchers have reported particle size  $\leq 300$  nm are ideal for oral drug delivery as they exhibit greater intestinal transport compared to larger particles.<sup>[41, 42]</sup> Furthermore, particle size data showed the controlled particle formation during the process as there was very low PDI for PNOB1 ( $0.141 \pm 0.03$ ) compared to unprocessed PTV ( $0.881 \pm 0.08$ ). The low PDI of PNOB1 reflects the presence of a homogeneous population within the system. A narrow particle size distribution is essential to prevent particle growth due to Ostwald ripening.<sup>[43, 44]</sup> The zeta-potential of PNOB1 was found to be  $-20.71 \pm 0.47$  mV compared to  $-0.81 \pm 0.01$  mV for unprocessed PTV. This can be explained by the adsorption of a TPGS-1000 which shifts the plane of shear to a larger distance from the particle surface results in a higher value of negative zeta potential. TPGS-1000 has a steric stabilization effect by its PEG part in the molecule. Several studies also supported the fact that a zeta potential of about -20 mV can also illustrate the long term stability of the system when steric stabilizers are used.<sup>[45]</sup>

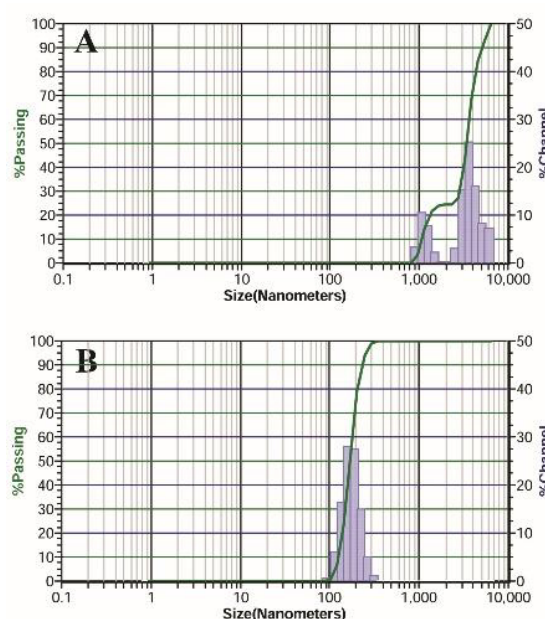


**Figure 7. Particle size analysis A) Unprocessed PTV B) PTV nanoparticles (PNOB1)**

#### **6.2.4.2 Scanning electron microscopy**

The surface morphology of optimized batch nanoparticles and unprocessed drug were observed under a scanning electron microscope (JSM-6010LA; JEOL, Tokyo, Japan). A sample was gold plated with a sputter coater, placed on aluminum plates, and observed at an acceleration voltage of 15 kV.

SEM images show the surface morphology of particles in which unprocessed drug presented as irregular rhombohedral shaped, with broad particle size distribution from 2 to 8  $\mu\text{m}$  (**Figure 8A**). While PNOB1 presented nearly amorphous and separated from each other (**Figure 8B**).

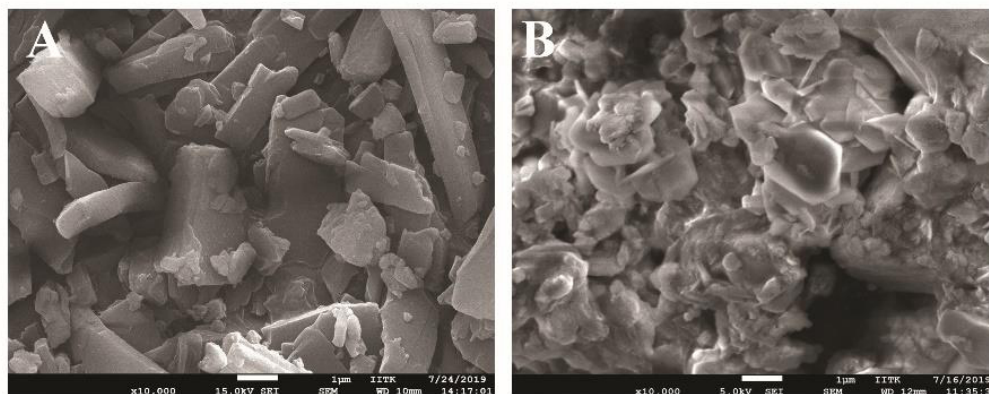


**Figure 8. SEM image of A) Unprocessed PTV and B) PTV nanoparticles (PNOB1)**

#### 6.2.4.3 Powder X-ray diffraction study

The X-ray diffraction (XRD) study was performed to evaluate the crystalline state of the powder sample. XRD pattern was recorded using an X-ray diffractometer (Xpert Pro MPD, Powder PAN analytical system, Almelo, Netherland) with Cu K $\alpha$  radiation (1.5405  $\text{\AA}$ ) at 40 mA, 35 kV and Xcelerator detector with diffracted beam monochromator. The degree of crystallinity and the relative degree of crystallinity was calculated using the following equations:<sup>[46, 47]</sup>

$$\text{Degree of Crystallinity (\%)} = \frac{A_c}{A_T} \times 100$$

Where ' $A_c$ ' is an area of crystalline peaks, ' $A_a$ ' is an area of amorphous peaks, and ' $A_T$ ' is the total area under the peak representing the area of amorphous peaks and area of crystalline peaks.

$$\text{Relative degree of crystallinity} = \frac{I}{I_{Drug}}$$

Where ' $I$ ' and ' $I_{Drug}$ ' represent the degree of crystallinity of formulation under investigation and pure drug respectively.

XRD analysis was employed to further investigate the crystalline state of the unprocessed drug and PNOB1. **Figure 9** showed essentially similar diffraction patterns and lattice spacing in unprocessed drug and PNOB1, suggesting that prepared nanoparticles did not undergo gross structural modification. Furthermore, the unprocessed drug showed intense peaks of crystallinity, whereas PTV nanoparticle (PNOB1) exhibited a halo pattern with less intense and denser peaks; indicating the

decrease in crystallinity or partial amorphization of the drug in its nano-form. The crystallinity for unprocessed drug and PNOB1 were found to be 83.02 % and 14.6 % respectively. Additionally, the relative degree of crystallinity of PNOB1 was found to be 0.176. These results confirm the amorphization of the drug in its nano form. Hence, improved drug dissolution is expected from the formulated optimized batch.<sup>[48]</sup> The conclusion drawn from the X-ray diffraction study was further verified by the DSC study.

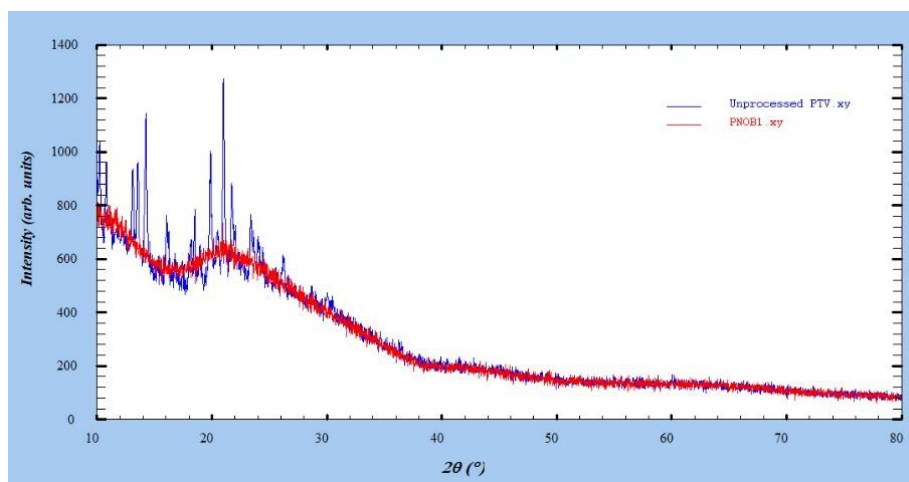


**Figure 9 Overlay XRD Plot for Unprocessed PTV and PTV nanoparticles (PNOB1)**

#### **6.2.4.4 Differential scanning calorimetry**

Differential scanning calorimetric analysis was performed on DSC-821e (Mettler Toledo, Switzerland). **Figure 10** presents the DSC thermograms of unprocessed drug and PNOB1. Unprocessed drug (**Figure 10A**) exhibited a sharp endotherm at 191.4 °C attributed to its crystalline nature. PNOB1 (**Figure 10B**) exhibited a slightly broad endotherm at 189.1 °C. Although the endotherm was observed at a lower temperature which can be attributed to the reduced particle size to nanometer as per Gibbs-Thomson equation or miscibility of drug with excipients.<sup>[49]</sup> The fact above demonstrated that there was a reduction in crystallinity during the processing. These results are consistent with XRD analysis and confirm to the amorphization of the drug in its nano-form.



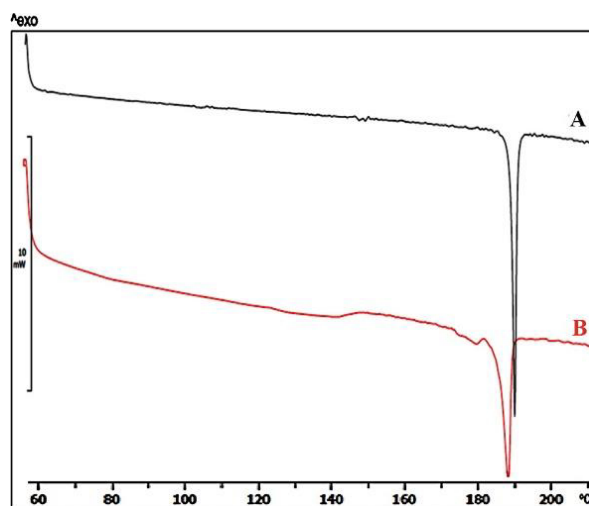


**Figure 10.** DSC spectra for (A) Unprocessed PTV and (B) PTV nanoparticles (PNOB1)

#### 6.2.4.5 Quantification of residual solvent

The residual solvent acetone in the optimized batch (PNOB1) was analyzed using Shimadzu GC-2014 with a headspace auto-sampler HT200H gas chromatograph (Shimadzu, Kyoto, Japan). a 1 mL sample was injected in the gaseous phase from blank followed by test preparation and standard solution. Peaks areas were used for obtaining quantitative data.<sup>[50]</sup>

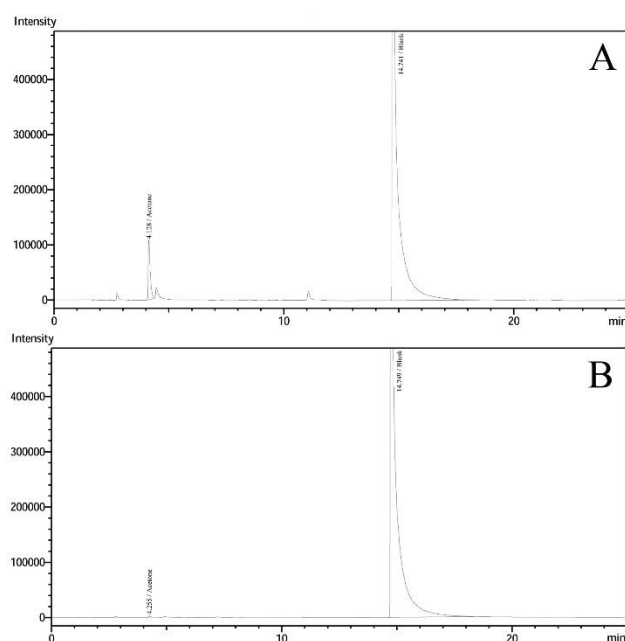


**Figure 11.** GC chromatogram of standard solutions of A) acetone and (B) PTV nanoparticles (PNOB1)

**Figure 11A** and **Figure 11B** depict the GC chromatograms for the standard solution of acetone and PNOB1 respectively. Retention time and peak area for the standard solution of acetone were 4.128 min and 646373.7  $\mu\text{Vsec}$  respectively, and for PNOB1 4.255 min and 10776.7  $\mu\text{Vsec}$  respectively.

The residual solvent (acetone) in the sample calculated from the peak area was found to be 82.7 ppm which was within the limit (< 5000 ppm). Therefore, it can be concluded that the freeze-drying technique was effective to eliminate acetone from PTV nanoparticles well below the prescribed limit.

#### 6.2.4.6 Saturation solubility

An excess amount of sample was dispersed in 10 mL of distilled water as well as in Phosphate buffer (PBS) pH 6.8. It was shaken at 50 RPM at room temperature for 24 h using an orbital shaking incubator (PSI-06, Patel Scientific Instrument, Ahmedabad). The filtered sample solutions were analyzed employing a UV-visible spectrophotometer (UV1800, Shimadzu, Kyoto, Japan) at 245 nm after appropriate dilution.

The PNOB1 saturation solubility showed 58.95-fold improvement ( $0.527 \pm 0.021$  vs.  $0.00894 \pm 0.0012$  mg/mL) in distilled water and 32.01-fold improvement ( $4.129 \pm 0.073$  vs.  $0.129 \pm 0.008$  mg/mL) in PBS pH 6.8 when compared with unprocessed PTV. These indicate significant improvement ( $p < 0.001$ ) of saturation solubility when PTV is formulated into nanoparticles. This phenomenon can be explained by Kelvin's equation which states that as the particle size decreases the dissolution pressure increases which leads to shifting the solubility equilibrium toward increased saturation solubility.<sup>[51]</sup> Moreover, Ostwald–Freundlich equation also explains that a decrease in particle size leads to an increase in dissolution pressure since strong curvature of nanoparticles.<sup>[52]</sup> PTV demonstrates almost negligible solubility in distilled water ( $0.00894 \pm 0.0012$  mg/mL) and PBS pH 6.8 ( $0.129 \pm 0.008$  mg/mL), resulting in its poor oral bioavailability. Improvement of solubility in the PBS pH 6.8 has the potential to improve its bioavailability.

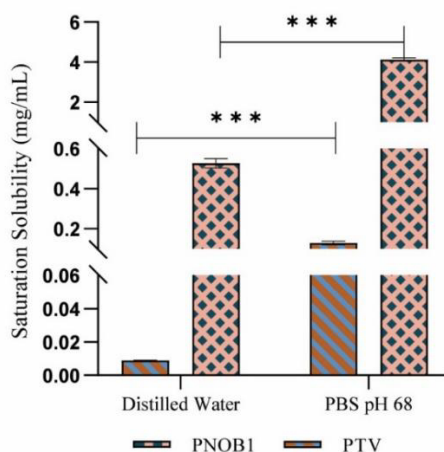


Figure 12. Saturation solubility study



## 6.3 Development of Tablet formulation containing PTV nanoparticles

### 6.3.1 Method of preparation of tablets

The formulations of the PTV tablets are shown in **Table 13**. The mass of each tablet prepared was calculated to have the same content of pitavastatin and a total mass equal to the marketed tablet. The tablet bulk mixture was prepared for 200 tablets. The freeze-dried PTV nanoparticles were mixed with tablet excipients using a polybag for 10 min. The tablets were prepared using direct compression using a 4 mm round shape flat-faced standard punch on a rotary tablet compression machine (Cemach Machineries Ltd, Ahmedabad). Batch code 'PNOB1-Tab' represents tablets containing optimized batch of nanoparticles, 'PTV-Tab' represents tablets containing unprocessed pure drug PTV, 'Marketed-Tab' represents conventional marketed formulation.

*Table 13. Composition of pitavastatin calcium tablet formulations*

Batch	Nanoparticles (PNOB1)	PTV (Unprocessed)	Excipients (mg)			
			AV	L-HPC	A	MS
PNOB1-Tab	2.34 mg	-	126.66	15	3	3
PTV-Tab	-	2.09 mg	126.91	15	3	3
Marketed-Tab		2.09 mg	*	*	*	*

AV= Avicel PH 102, L-HPC= Low-Substituted Hydroxypropyl Cellulose, A= Aerosil, MS = magnesium stearate, \* not known. Assay of PNOB1 =  $89.47 \pm 0.29$  %, 2.09 mg pitavastatin calcium is equivalent to 2 mg pitavastatin. Each tablet weight 150 mg, Tablet was compressed by direct compression using a 4 mm round shape standard punch on a rotary tablet compression machine.

### 6.3.2 Evaluation of tablet formulation

The pre and post-compression parameters were evaluated according to official standards. As presented in **Table 14**, the experimental values of pre-compression tests indicated that bulk mixtures possess good flow properties and packing ability. The post-compression analysis value shows that the prepared and marketed tablets well within the official standards as per the USP 40–NF 35.<sup>[53]</sup>

*Table 14. Pre and post-compression parameters of tablet formulations*

Sample	Pre-compression				Post-compression			
	Hausner's ratio	Carr's Index	Angle of repose ( $\theta$ )	Hardness (kg-cm)	Weight Variation (mg)	Friability (%)	Disintegration time (sec)	Assay (%)
PNOB1-Tab	$1.12 \pm 0.03$	$10.53 \pm 0.92$	$25.31 \pm 1.07$	$4.12 \pm 0.098$	$151.28 \pm 3.9$	$0.012 \pm 0.002$	$34.67 \pm 5.73$	$99.63 \pm 0.364$
PTV-Tab	$1.09 \pm 0.13$	$7.89 \pm 0.91$	$27.76 \pm 1.73$	$4.2 \pm 0.13$	$150.83 \pm 4.02$	$0.011 \pm 0.002$	$33 \pm 4.32$	$99.37 \pm 0.583$
Marketed-Tab	-	-	-	-	-	-	$125.67 \pm 4.92$	$99.12 \pm 0.493$

### 6.3.3 *In-vitro* drug release study

The results of the *in-vitro* dissolution test reported in **Figure 13**. The average percent cumulative drug release (%CDR) at 45 min of PNOB1-Tab, PTV-Tab batches, and marketed tablets were found to be  $98.15 \pm 1.29 \%$ ,  $66.80 \pm 1.29 \%$ , and  $80.94 \pm 5.62 \%$  respectively. The tablet batches with  $\geq 80 \%$  CDR of the label claim PTV at 45 min considered acceptable.<sup>[16]</sup> For PNOB1-Tab and marketed tablets were within acceptance criteria while PTV-Tab falls short in drug release criteria.

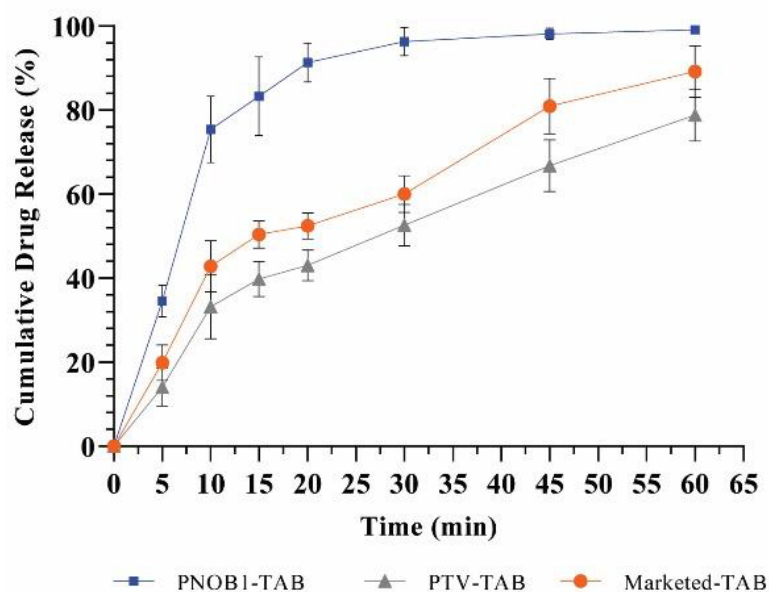


**Figure 13.** Dissolution curve of prepared batches & marketed tablets

### 6.3.4 Drug release kinetic

The release mechanisms of the formulations were evaluated by different *in-vitro* kinetics models: the zero-order, first-order.<sup>[54]</sup> The results of drug release kinetic shows that first-order  $R^2$  value for PNOB1-Tab, PTV-Tab, and Marketed-Tab were  $0.9760 \pm 0.013$ ,  $0.9618 \pm 0.010$ , and  $0.9558 \pm 0.007$  respectively which was found to be higher than zero-order  $r^2$  value indicates that they follow the first-order drug release kinetics. The first-order process of drug release is expected for conventional solid dosage forms.<sup>[55]</sup> Additionally, the first-order drug release constant ( $K_1$ ) for PNOB1-Tab, PTV-Tab, and Marketed-Tab were found to be  $0.116 \pm 0.016$ ,  $0.028 \pm 0.005$ , and  $0.040 \pm 0.006$  respectively, which indicates that PNOB1-Tab demonstrates faster drug release compared to PTV-Tab and Marketed-Tab.

The similarity factor ( $f_2$ ) was found to be 28.902 for PNOB1-Tab and 51.486 for PTV-Tab compared to Marketed-Tab while 22.874 for PNOB1-Tab compared to PTV-Tab. The  $f_2$  values<sup>[56]</sup> less than 50 indicate dissimilarity and greater than 50 indicate similarity

between the release profile of drug from test and reference formulation. In this context, results indicate the dissimilarity of PNOB1-Tablets compared to Marketed-Tablets and PTV-Tablets. Conversely, PTV-Tablets shows marginal similarity with Marketed-Tablets.

### 6.3.5 Dissolution efficiency and Mean dissolution time

The DE% and MDT allows the comparison of drug dissolution profiles.<sup>[57]</sup> Dissolution efficiency is related to the real amount of drug dissolved in the dissolution medium and thus, lead to a better prognostic for *in-vivo* performance.<sup>[57]</sup> PNOB1-Tab ( $85.2161 \pm 2.403$ ) shows the highest DE% compared to PTV-Tab ( $63.5882 \pm 2.524$ ) and Marketed-Tab ( $67.0871 \pm 0.984$ ). Besides, the MDT of formulations was calculated as it is a measure of the rate of the dissolution process. The MDT for PNOB1-Tab ( $8.87 \pm 1.44$ ) was found to be lowest compared to PTV-Tab ( $21.85 \pm 1.51$ ) and Marketed-Tab ( $19.75 \pm 0.59$ ). These results supported by the fact that the lower the MDT, the faster the release rate which could lead to better *in-vivo* performance.<sup>[57]</sup> The analysis of variance (ANOVA) also revealed a statistical difference ( $p < 0.05$ ) between the formulations (Table 15). Post-hoc Tukey test also demonstrated the significant ( $p < 0.05$ ) improvement in DE% and MDT of PNOB1-Tab compared to PTV-Tab and Marketed tablets.

**Table 15. Dissolution efficiency and mean dissolution time**

Parameter	PNOB1-Tab	PTV-Tab	Marketed-Tab
DE (%)	$85.2161 \pm 2.403^{*,\#}$	$63.5882 \pm 2.524^{ns}$	$67.0871 \pm 0.984$
MTD (h)	$8.87 \pm 1.44^{*,\#}$	$21.85 \pm 1.51^{ns}$	$19.75 \pm 0.59$

Data expressed as Average  $\pm$ SD; n = 6

PNOB1-Tab and PTV-Tab were compared to Marketed-Tab. One-way ANOVA followed by a Tukey's multiple comparison test: ns = not significant; \*  $p < 0.05$  compared to Marketed-TAB; #  $p < 0.05$  compared to PTV-Tab

## 6.4 In-vivo pharmacokinetic study

The *In-vivo* pharmacokinetic experiment protocol was approved by the Institutional Animal Ethics Committee (CPSEA/VBT/IAEC/15/01/75). The pharmacokinetics of the formulated nanoparticle-loaded tablet (PNOB1-Tab) was compared to unprocessed drug-loaded tablet (PTV-Tab) and marketed tablet (Marketed-Tab) in Wistar albino rats.

### 6.4.1 Animals and dosing

The animals were housed at a temperature of  $25 \pm 3^\circ\text{C}$  and  $60 \pm 5\%\text{RH}$ . They were kept in wire cages with free access to feed and water ad libitum. The animals for the study

---

were subjected to overnight fasting. The animals weighing 150-200 g were divided into 3 groups; PNOB1-Tab, PTV-Tab, and Marketed-Tab of 6 animals. Animals were treated orally with a dose of 400 µg/kg PTV of body weight. The samples were suspended in 0.5 % carboxymethyl cellulose (CMC) before administration. Blood samples (0.2 mL) were periodically collected from the retro-orbital plexus in ethylenediaminetetraacetic acid (EDTA) containing tube at 0.25, 0.5, 1, 1.5, 2, 4, 6, 8, 12, and 24 h after oral administration. The equal volume of normal saline was injected after each sampling to maintain the uniform blood volume. Plasma was separated by centrifugation at 5000 RPM for 10 min (3K30; Sigma Laborzentrifugen) and stored at -20°C until further analysis.

#### 6.4.2 Quantification of PTV in plasma samples

The plasma (100 µl) was extracted with 100 µl acetonitrile and 200 µl *tert*-butyl-methyl ether and vortexed. Each sample was then centrifuged at 5000 RPM for 15 min. The obtained supernatant was transferred to another clean tube and was evaporated to dryness under a gentle stream of nitrogen. The residue was dissolved in 200 µl of the HPLC mobile phase and an aliquot of 20 µl was injected into the HPLC system to quantify the amount of drug. A mobile phase consisted of acetonitrile, water, and tetrahydrofuran in 43:55:2 v/v/v proportions with pH 3.0, maintained at a flow rate of 1.2 mL/min. The C<sub>18</sub> analytical column (5.0 µm; 250 × 4.6 mm) (Kromasil, Phenomenex, USA) was employed for the estimation. PTV was quantified at 249 nm using a PDA detector. Calibration curve was obtained from 10 to 1000 ng/ml ( $r^2 = 0.9979$ ).

#### 6.4.3 Pharmacokinetic data analysis

The pharmacokinetic parameters T<sub>max</sub>, C<sub>max</sub>, area under the curve (AUC), elimination half-life (t<sub>1/2</sub>), mean residence time (MRT) were determined by non-compartmental analysis using *PKSolver 2.0*.<sup>[58]</sup> The relative bioavailability (F) was calculated by the following equation:

$$\text{Relative Bioavailability (F)} = \frac{AUC_{\text{test}}}{AUC_{\text{Reference}}} \times 100 \dots\dots\dots (5)$$

#### 6.4.4 Results of In-vivo pharmacokinetic study

The mean plasma drug concentration vs. time profile for the single oral administration of PNOB1-Tab, PTV-Tab, and Marketed-Tab is shown in **Figure 14**, and **Table 16** shows the calculated pharmacokinetic parameters. The C<sub>max</sub> of PNOB1-Tab showed statistically significant improvement of 1.43-fold over the Marketed-Tab and 1.53-

fold, over the PTV-Tab (**Table 16**). Against the expectation, a left shift in the  $T_{\max}$  for PNOB1-Tab was not observed, and similar  $T_{\max}$  values were observed for all three formulations. This may be attributed to both active as well passive absorptions of PTV from the gastrointestinal tract.

Furthermore, PNOB1-Tab formulation shows significant improvement in MRT and half-life compared to PTV-Tab and Marketed Tab indicates a faster release of PTV from the formulation. The  $AUC_{0-\infty}$  of PNOB1-Tab ( $7310.37 \pm 242.71$ ) was found to be higher than Marketed Tab ( $4155.91 \pm 137.98$ ) and PTV-Tab ( $3869.41 \pm 128.47$ ). This indicated that PNOB1-Tab enhanced PTV bioavailability by 1.76-fold when compared to Marketed Tab. Further, the PNOB1-Tab also shows a 1.89-fold improvement in bioavailability over PTV-Tab. The reason for this improvement in bioavailability may be due to the formulation of PTV nanoparticle (PNOB1-Tab) which reduces the particle size, enhance apparent solubility, and release rate of PTV compared to tablets containing unprocessed PTV.<sup>[59]</sup> The mechanisms contributed to the improved absorption could be majorly summarized as three points: Firstly, the amorphous state of PNOB1 exhibits higher solubility and faster dissolution rate due to the higher inner energy.<sup>[48]</sup> Therefore when dosed through the oral route, the nanoparticle formulation rate revealed more significant effects on enhancing bioavailability than the unprocessed PTV provided the high energy state could be kept in the GIT.<sup>[60]</sup> Secondly, nanoparticles possess general mucoadhesion to biological mucosa including GI mucosa.<sup>[61]</sup> The mucoadhesion of drug nanoparticles to GI mucosa leads to a higher concentration gradient and also a prolonged retention time.<sup>[62]</sup> Lastly, the ability of drug nanoparticles to enhance bioavailability could be partly attributed to the inhibition effects of coated stabilizer (TPGS 1000) on the efflux function of the P-glycoprotein (P-gp) which is located in the apical membranes of intestinal absorptive cells.<sup>[63]</sup>

**Table 16. In-vivo Pharmacokinetic parameters**

PK Parameters	PNOB1-Tab	Marketed-Tab	PTV-Tab
$T_{1/2}$ (h)	$10.86 \pm 0.05^{*,\#}$	$9.16 \pm 0.03$	$9.20 \pm 0.02^{ns}$
$T_{\max}$ (h)	1.00	1.00	1.00
$C_{\max}$ (ng/ml)	$798.05 \pm 26.50^{*,\#}$	$558.56 \pm 18.54$	$519.47 \pm 17.25^*$
$AUC_{0-\infty_{obs}}$ (ng/ml*h)	$7310.37 \pm 242.71^{*,\#}$	$4155.91 \pm 137.98$	$3869.41 \pm 128.47^{ns}$
$MRT_{0-\infty_{obs}}$ (h)	$15.96 \pm 0.02^{*,\#}$	$13.32 \pm 0.14$	$13.21 \pm 0.02^{ns}$

Data expressed as mean  $\pm$ SD; n = 6

PNOB1-Tab and PTV-Tab were compared to Marketed-Tab. One-way ANOVA followed by a Tukey's multiple comparison test: ns = not significant; \*  $p < 0.05$ , compared to Marketed-Tab; #  $p < 0.05$  compared to PTV-Tab.

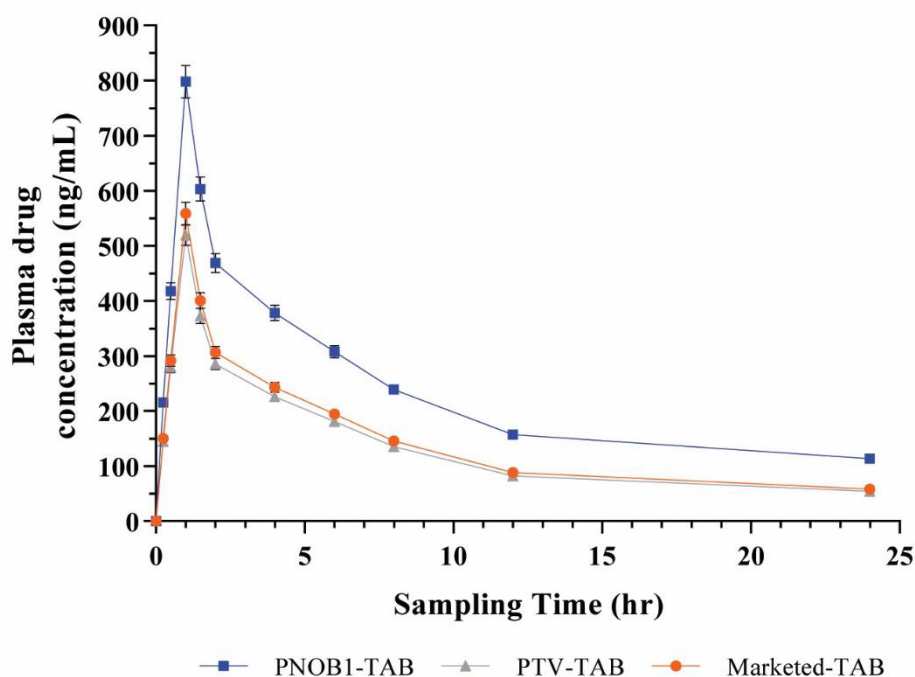


Figure 14. Mean plasma drug concentration–time profile curve

## 6.5 Stability study

The stability study of optimized PNOB1 was carried out at different conditions shown in **Table 17**. There was a non-significant alteration in particle size, PDI, as well as zeta potential compared to the initial sample, indicate the stability of optimized nanoparticles over 3 months. These results indicated that PNOB1 was physically stable which might be due to the presence of TPGS-1000 serve as inhibitors of particle growth by surface coating.<sup>[37]</sup> Also, stability could attribute to freeze-drying which plays an important role to uphold the stability of nanoparticles.<sup>[64]</sup> Additionally, the short term stability of the tablet containing these nanoparticles was also evaluated as shown in **Table 18**. A physicochemical property does not show any significant difference from the initial sample. Moreover, *in-vitro* dissolution results of the three months' stability sample showed nearly similar drug release profiles between initial samples. The formulation also able to maintain 50% of drug release within ~6 min and 80% within ~14 min during the stability period.

Table 17. Stability study of PTV nanoparticles (PNOB1)

Observation Parameters	Initial	At 4 °C	At 25 °C
		After 90 day	
Particle size (nm)	207.8 ± 3.72	218.2 ± 12.9	221.2 ± 16.1
Poly-dispersity index	0.102 ± 0.03	0.149 ± 0.36	0.128 ± 0.09
Zeta potential (mV)	-20.71 ± 0.47	-21.27 ± 0.71	-21.87 ± 1.02

Data expressed as mean ±SD; n = 3

**Table 18 Stability study PTV nanoparticles loaded-tablet (PNOB1-Tab)**

Observation Parameters	Initial	25 ± 2 °C/ 60 ± 5% RH			40 ± 2 °C/ 75 ± 5% RH		
		30 day	60 day	90 day	30 day	60 day	90 day
Hardness (Kg-cm)	4.12 ± 0.10	4.2 ± 0.09	4.22 ± 0.10	4.24 ± 0.12	4.22 ± 0.19	4.4 ± 0.18	4.46 ± 0.21
Friability (%)	0.058 ± 0.019	0.053 ± 0.019	0.052 ± 0.016	0.047 ± 0.015	0.049 ± 0.015	0.046 ± 0.016	0.042 ± 0.014
Disintegration Time (sec)	34.67 ± 5.73	35.33 ± 7.13	35.67 ± 8.06	38.67 ± 6.94	36.67 ± 7.32	39.67 ± 8.18	45.67 ± 8.06
Assay (%)	99.63 ± 0.36	99.52 ± 0.40	99.2 ± 0.37	98.31 ± 0.69	99.43 ± 1.17	98.33 ± 1.37	97.03 ± 1.14
CDR at 45 min (%)	98.16 ± 1.29	98.45 ± 1.33	98.32 ± 1.71	97.99 ± 1.56	99.19 ± 1.59	97.46 ± 1.44	96.90 ± 2.49
T <sub>50</sub> (min)	6.10 ± 0.93	6.11 ± 0.91	6.09 ± 0.90	6.12 ± 0.95	6.18 ± 0.84	6.18 ± 0.95	6.34 ± 0.81
T <sub>80</sub> (min)	14.16 ± 2.15	14.18 ± 2.11	14.13 ± 2.10	14.22 ± 2.20	14.36 ± 1.96	14.35 ± 2.22	14.72 ± 1.87
f <sub>2</sub>	-	99.392	98.734	97.891	92.358	97.239	85.797

Data expressed as mean ±SD; n = 3

## 7 ACHIEVEMENTS WITH RESPECT TO OBJECTIVES

### **Objective-1: Development and evaluation of Pitavastatin nanoparticle using Design of experiment approach.**

In the present study, the emulsion solvent evaporation followed by freeze-drying technique was effectively employed for the preparation of nanoparticles. Various process and formulation variables were successfully evaluated and screened using the Plackett-Burman design. A response surface optimization approach, Box-Behnken Design, was effectively used to study the effects of independent variables on desired attributes. The optimized nanoparticles showed a narrow particle size distribution with acceptable zeta potential. SEM and XRD study confirmed a decrease in crystallinity and amorphization of the drug in its nano form.

### **Objective-2: Enhance solubility and dissolution rate of poorly soluble drug (Pitavastatin calcium).**

PTV demonstrates almost negligible solubility in distilled water ( $0.00894 \pm 0.0012$  mg/mL) and PBS pH 6.8 ( $0.129 \pm 0.008$  mg/mL), resulting in its poor oral bioavailability. The optimized batch of PTV nanoparticle showed 58.95-fold improvement in saturation solubility ( $0.527 \pm 0.021$  vs.  $0.00894 \pm 0.0012$  mg/mL) in distilled water and 32.01-fold improvement ( $4.129 \pm 0.073$  vs.  $0.129 \pm 0.008$  mg/mL) in PBS pH 6.8 when compared with unprocessed PTV. These indicate significant improvement ( $p < 0.001$ ) of saturation solubility when PTV is formulated into nanoparticles.



---

The tablets containing PTV nanoparticles showed significant improvement in *in-vitro* drug release compared to tablets containing unprocessed PTV as well as marketed tablets. The first-order drug release constant ( $K_1$ ) for PNOB1-Tab, PTV-Tab, and Marketed-Tab were found to be  $0.116 \pm 0.016$ ,  $0.028 \pm 0.005$ , and  $0.040 \pm 0.006$  respectively, which indicates that PNOB1-Tab demonstrates faster drug release compared to PTV-Tab and Marketed-Tab. The highest DE% was observed for PNOB1-Tab ( $85.2161 \pm 2.403$ ) compared to PTV-Tab ( $63.5882 \pm 2.524$ ) and Marketed-Tab ( $67.0871 \pm 0.984$ ). The MDT for PNOB1-Tab ( $8.87 \pm 1.44$ ) was found to be lowest compared to PTV-Tab ( $21.85 \pm 1.51$ ) and Marketed-Tab ( $19.75 \pm 0.59$ ). These results supported by the fact that the lower the MDT, the faster the release rate which could lead to better *in-vivo* performance.<sup>[57]</sup>

**Objective-3: To study in-vivo pharmacokinetic behavior of formulation containing developed Pitavastatin nanoparticle.**

The *in-vivo* pharmacokinetic study of prepared nanoparticle loaded tablets showed a significant improvement in bioavailability than unprocessed drug-loaded and marketed tablets after single-dose oral administration to rats. The  $C_{max}$  of PNOB1-Tab showed statistically significant improvement of 1.43-fold over the Marketed-Tab and 1.53-fold, over the PTV-Tab.

PNOB1-Tab formulation shows significant improvement in MRT and half-life compared to PTV-Tab and Marketed Tab indicates a faster release of PTV from the formulation. The  $AUC_{0-\infty}$  of PNOB1-Tab ( $7310.37 \pm 242.71$ ) was found to be higher than Marketed Tab ( $4155.91 \pm 137.98$ ) and PTV-Tab ( $3869.41 \pm 128.47$ ). This indicated that PNOB1-Tab enhanced PTV bioavailability by 1.76-fold when compared to Marketed Tab. Further, the PNOB1-Tab also shows a 1.89-fold improvement in bioavailability over PTV-Tab. The reason for this improvement in bioavailability attributed to the formulation of PTV nanoparticle which reduces the particle size enhances apparent solubility, and release rate of PTV compared to tablets containing unprocessed PTV.<sup>[59]</sup>

Moreover, the stability study results proved that optimized nanoparticles as well as nanoparticles loaded tablets were stable over three months.

## 8 CONCLUSION

We showed that the emulsion solvent evaporation techniques successfully generated PTV nanoparticles stabilized by TPGS-1000. Various process and formulation



---

variables were successfully evaluated and screened using the Plackett-Burman design. A response surface optimization approach, Box-Behnken Design, was effectively used to study the effects of independent variables on desired attributes. The optimized nanoparticles showed a narrow particle size distribution with acceptable zeta potential. SEM and XRD study confirmed a decrease in crystallinity and amorphization of the drug in its nano form. The apparent solubility of prepared nanoparticle increased by 58.95-fold in distilled water and 32.01-fold in PBS pH 6.8. Further, this result also supported the dissolution profile of nanoparticle loaded tablet which shows significant high dissolution efficacy and low mean dissolution time compared to the conventional product. The prepared nanoparticle loaded tablet showed a significant improvement in bioavailability than unprocessed drug-loaded and marketed tablets after single-dose oral administration to rats. The optimized nanoparticles as well as nanoparticles loaded tablets were found to be stable over 3 months. All these findings signify that the PTV nanoparticle loaded tablets can successfully employ in improving dissolution and thereby oral bioavailability of PTV.

## 9 LIST OF PUBLICATIONS AND PRESENTATIONS

- 1 Ramani VD, Jani GK, Sen AK, Sailor GU, Sutariya VB, "Development and validation of RP-HPLC method for pitavastatin calcium in bulk and formulation using experimental design". Journal of Applied Pharmaceutical Science. 2019, 9(10), 075-083, ISSN 2231-3354. <https://doi.org/10.7324/JAPS.2019.91010> <sup>[18]</sup>  
Journal Scopus listing link: <https://www.scopus.com/sourceid/21100236605>
- 2 Ramani VD, Jani GK, Sailor GU, "Application of Plackett-Burman Design for Screening of Factors Affecting Pitavastatin Nanoparticle Formulation Development". Folia Medica (Plovdiv), 2020. ISSN:0204-8043.<sup>[65]</sup> [Article status: Accepted, Under Copy editing]  
Journal Scopus listing link: <https://www.scopus.com/sourceid/39363>

### 9.1 International Poster Presentations

- 1 Presented poster on "Simplex centroid design aided mobile phase composition optimization for HPLC method development of Pitavastatin in Bulk and Formulation" in the 2018 AAPS PharmSci 360 held on November 4-7, 2018 at Washington DC, USA.
- 2 Secured First Rank in poster presentation competition in 5th International Conference "Advance in topical drug delivery: Global perspective and

---

contribution of India academic research held on May 11, 2017, at Shree Dhanvantary Pharmacy College, Kim, Surat, Gujarat, India.

## 10 REFERENCES

1. Ahmad H, Cheng-Lai A, "Pitavastatin: a new HMG-CoA reductase inhibitor for the treatment of hypercholesterolemia". *Cardiol Rev.* **2010**, 18(5), 264-267.
2. Van Der Schaaf PA, Blatter F, Szelagiewicz M, Schoening K-U, inventors Crystalline forms of pitavastatin calcium. USA patent US8557993B2. **2013**.
3. PubChem Compound Summary for CID 11251522, Pitavastatin calcium [Internet]. PubChem. 2020 [cited Jan. 13, 2020]. Available from: <https://pubchem.ncbi.nlm.nih.gov/compound/Pitavastatin-calcium>.
4. USFDA Cfdear. Non-Clinical Review: NDA 208379 (Class 2 Resubmission) Pitavastatin Magnesium. USA: 2015 2083790rig15000.
5. Pitavastatin calcium [Internet]. [cited Jan. 13, 2018]. Available from: <https://www.drugbank.ca/salts/DBSALT000140>.
6. Charalabidis A, Sfouni M, Bergström C, Macheras P, "The Biopharmaceutics Classification System (BCS) and the Biopharmaceutics Drug Disposition Classification System (BDDCS): Beyond guidelines". *Int J Pharm.* **2019**, 566, 264-281.
7. Hirano M, Maeda K, Matsushima S, Nozaki Y, Kusuhara H, Sugiyama Y, "Involvement of BCRP (ABCG2) in the biliary excretion of pitavastatin". *Mol Pharmacol.* **2005**, 68(3), 800-807.
8. Hirano M, Maeda K, Shitara Y, Sugiyama Y, "Drug-drug interaction between pitavastatin and various drugs via OATP1B1". *Drug Metab Dispos.* **2006**, 34(7), 1229-1236.
9. Lin Y, Shen Q, Katsumi H, Okada N, Fujita T, Jiang X, et al., "Effects of Labrasol and other pharmaceutical excipients on the intestinal transport and absorption of rhodamine123, a P-glycoprotein substrate, in rats". *Biol Pharm Bull.* **2007**, 30(7), 1301-1307.
10. Varma MV, Ashokraj Y, Dey CS, Panchagnula R, "P-glycoprotein inhibitors and their screening: a perspective from bioavailability enhancement". *Pharm Res.* **2003**, 48(4), 347-359.
11. Nirmala D, Chakradhar PA, Sudhakar M, "Preparation and characterization of Pitavastatin solid dispersions". *Res J Pharm Technol.* **2016**, 9(5), 555-558.
12. Van Der Schaaf PA, Blatter F, Szelagiewicz M, Schoening K-U, inventors; Nissan Chemical Corp, assignee. Crystalline forms of pitavastatin calcium. USA patent US20180346425A1. **2018** Dec 6.
13. Ahmed TA, Bawazir AO, Omar AM, Safo MK, inventors; King Abdulaziz University, assignee. Mucoadhesive buccal film having a dual release carrier system. US patent 10709662. **2020** July 14.
14. Mahalakshmi K. Formulation and in-vitro evaluation of Liquid and solid self microemulsifying Drug delivery system of pitavastatin Calcium. Chennai: Dr MGR Medical University; 2018.
15. Mauludin R, Müller RH, Keck CM, "Development of an oral rutin nanocrystal formulation". *Int J Pharm.* **2009**, 370(1-2), 202-209.
16. Commission IP. Indian Pharmacopoeia. Ghaziabad: Government of India, Ministry of Health & Family Welfare; 2018.

17. Dwivedi SD, Patel DJ, Shah AP, Khera B, inventors; world patent, assignee. Pitavastatin calcium and process for its preparation patent WO2012025939A1. **2015**.
18. Ramani VD, Jani GK, Sen AK, Sailor GU, Sutariya VB, "Development and validation of RP-HPLC method for pitavastatin calcium in bulk and formulation using experimental design". *J Appl Pharm Sci*. **2019**, 9(10), 075-083.
19. IR Spectrum Table & Chart [Internet]. sigmaaldrich- Merck KGaA. 2020 [cited 03-03-2020]. Available from: <https://www.sigmaaldrich.com/technical-documents/articles/biology/ir-spectrum-table.html>.
20. Gomas AR, Ram PR, Srinivas N, Sriramulu J, "Degradation pathway for pitavastatin calcium by validated stability indicating UPLC method". *Am J Analyt Chem*. **2010**, 1(2), 83.
21. Kojima J, Fujino H, Yosimura M, Morikawa H, Kimata H, "Simultaneous determination of NK-104 and its lactone in biological samples by column-switching high-performance liquid chromatography with ultraviolet detection". *J Chromatogr B Biomed Sci Appl*. **1999**, 724(1), 173-180.
22. Panchal HJ, Suhagia BN, Patel MM, Patel BH, "Estimation of pitavastatin calcium in tablet dosage forms by column liquid chromatography and ultraviolet spectrophotometry". *J AOAC Int*. **2008**, 92(1), 158-164.
23. Beg S, Kohli K, Swain S, Hasnain MS, "Development and validation of RP-HPLC method for quantitation of amoxicillin trihydrate in bulk and pharmaceutical formulations using Box-Behnken experimental design". *J Liq Chromatogr Relat Technol*. **2012**, 35(3), 393-406.
24. Berridge JC, "Techniques for the automated optimization of HPLC separations". *Trends Analyt Chem*. **1984**, 3(1), 5-10.
25. Hasnain MS, Rao S, Singh MK, Vig N, Gupta A, Ansari A, et al., "Development and validation of LC–MS/MS method for the quantitation of lenalidomide in human plasma using Box–Behnken experimental design". *Analyst*. **2013**, 138(5), 1581-1588.
26. Srinubabu G, Raju CA, Sarath N, Kumar PK, Rao JS, "Development and validation of a HPLC method for the determination of voriconazole in pharmaceutical formulation using an experimental design". *Talanta*. **2007**, 71(3), 1424-1429.
27. ICH Guideline HT, "Validation of analytical procedures: text and methodology Q2 (R1)(2005)". Website: <http://www.ich.org/cache/compo/363-272-1.html>. **2010**.
28. Kakran M, Sahoo NG, Tan I-L, Li L, "Preparation of nanoparticles of poorly water-soluble antioxidant curcumin by antisolvent precipitation methods". *J Nanopart Res*. **2012**, 14(3), 757.
29. Kocbek P, Baumgartner S, Kristl J, "Preparation and evaluation of nanosuspensions for enhancing the dissolution of poorly soluble drugs". *Int J Pharm*. **2006**, 312(1-2), 179-186.
30. Guo Y, Luo J, Tan S, Otieno BO, Zhang Z, "The applications of Vitamin E TPGS in drug delivery". *Eur J Pharm Sci*. **2013**, 49(2), 175-186.
31. Joye IJ, McClements DJ, "Production of nanoparticles by anti-solvent precipitation for use in food systems". *Trends Food Sci Technol*. **2013**, 34(2), 109-123.
32. Zhang J-Y, Shen Z-G, Zhong J, Hu T-T, Chen J-F, Ma Z-Q, et al., "Preparation of amorphous cefuroxime axetil nanoparticles by controlled nanoprecipitation method without surfactants". *Int J Pharm*. **2006**, 323(1-2), 153-160.
33. Cushing BL, Kolesnichenko VL, O'Connor CJ, "Recent advances in the liquid-phase syntheses of inorganic nanoparticles". *Chem Rev*. **2004**, 104(9), 3893-3946.

34. Langer K, Balthasar S, Vogel V, Dinauer N, Von Briesen H, Schubert D, "Optimization of the preparation process for human serum albumin (HSA) nanoparticles". *Int J Pharm.* **2003**, 257(1-2), 169-180.
35. Plackett RL, Burman JP, "The design of optimum multifactorial experiments". *Biometrika.* **1946**, 33(4), 305-325.
36. Fu T, Gu X, Liu Q, Peng X, Yang J, "Study on the stabilization mechanisms of wet-milled cepharanthine nanosuspensions using systematical characterization". *Drug Dev Ind Pharm.* **2020**, 46(2), 200-208.
37. Ahuja BK, Jena SK, Paidi SK, Bagri S, Suresh S, "Formulation, optimization and in vitro–in vivo evaluation of febuxostat nanosuspension". *Int J Pharm.* **2015**, 478(2), 540-552.
38. Zacour BM, Drennen III JK, Anderson CA, "Development of a fluid bed granulation design space using critical quality attribute weighted tolerance intervals". *J Pharm Sci.* **2012**, 101(8), 2917-2929.
39. Loh ZH, Samanta AK, Heng PWS, "Overview of milling techniques for improving the solubility of poorly water-soluble drugs". *Asian J Pharm Sci.* **2015**, 10(4), 255-274.
40. Ramasamy T, Tran TH, Choi JY, Cho HJ, Kim JH, Yong CS, et al., "Layer-by-layer coated lipid–polymer hybrid nanoparticles designed for use in anticancer drug delivery". *Carbohydr Polym.* **2014**, 102, 653-661.
41. Banerjee A, Qi J, Gogoi R, Wong J, Mitragotri S, "Role of nanoparticle size, shape and surface chemistry in oral drug delivery". *J Control Release.* **2016**, 238, 176-185.
42. Desai MP, Labhasetwar V, Amidon GL, Levy RJ, "Gastrointestinal uptake of biodegradable microparticles: effect of particle size". *Pharm Res.* **1996**, 13(12), 1838-1845.
43. Danaei M, Dehghankhold M, Ataei S, Hasanzadeh Davarani F, Javanmard R, Dokhani A, et al., "Impact of particle size and polydispersity index on the clinical applications of lipidic nanocarrier systems". *Pharmaceutics.* **2018**, 10(2), 57.
44. Verma S, Kumar S, Gokhale R, Burgess DJ, "Physical stability of nanosuspensions: investigation of the role of stabilizers on Ostwald ripening". *Int J Pharm.* **2011**, 406(1-2), 145-152.
45. Chen L, Wang Y, Zhang J, Hao L, Guo H, Lou H, et al., "Bexarotene nanocrystal—Oral and parenteral formulation development, characterization and pharmacokinetic evaluation". *Eur J Pharm Biopharm.* **2014**, 87(1), 160-169.
46. Ribotta PD, Cuffini S, León AE, Añón MC, "The staling of bread: an X-ray diffraction study". *Eur Food Res Technol.* **2004**, 218(3), 219-223.
47. Saadiah M, Zhang D, Nagao Y, Muzakir S, Samsudin A, "Reducing crystallinity on thin film based CMC/PVA hybrid polymer for application as a host in polymer electrolytes". *J Non Cryst Solids.* **2019**, 511, 201-211.
48. Gao L, Liu G, Wang X, Liu F, Xu Y, Ma J, "Preparation of a chemically stable quercetin formulation using nanosuspension technology". *Int J Pharm.* **2011**, 404(1-2), 231-237.
49. Jackson CL, McKenna GB, "The melting behavior of organic materials confined in porous solids". *J Chem Phys.* **1990**, 93(12), 9002-9011.
50. Siddiqui MR, Singh R, Bhatnagar A, Kumar J, Chaudhary M, "Determination of residual solvents in docetaxel by headspace gas chromatography". *Arab J Chem.* **2017**, 10(2), S2479-S2484.
51. Buckton G, Beezer AE, "The relationship between particle size and solubility". *Int J Pharm.* **1992**, 82(3), R7-R10.

- 
52. Shchekin A, Rusanov A, "Generalization of the Gibbs–Kelvin–Köhler and Ostwald–Freundlich equations for a liquid film on a soluble nanoparticle". *The Journal of chemical physics*. **2008**, 129(15), 154116.
  53. United States Pharmacopeia - National Formulary. USP 40-NF 35 ed: United States Pharmacopeial Convention; 2017.
  54. Costa P, Lobo JMS, "Modeling and comparison of dissolution profiles". *Eur J Pharm Sci*. **2001**, 13(2), 123-133.
  55. Ishii K, Saitou Y, Yamada R, Itai S, Nemoto M, "Novel approach for determination of correlation between in vivo and in vitro dissolution using the optimization technique". *Chem Pharm Bull (Tokyo)*. **1996**, 44(8), 1550-1555.
  56. Moore JW, Flanner HH, "Mathematical comparison of dissolution profiles". *Pharm Technol*. **1996**, 20(6), 64-74.
  57. Oliveira ÉDFS, Azevedo RdCP, Bonfilio R, Oliveira DBd, Ribeiro GP, Araújo MBd, "Dissolution test optimization for meloxicam in the tablet pharmaceutical form". *Braz J Pharm Sci*. **2009**, 45(1), 67-73.
  58. Zhang Y, Huo M, Zhou J, Xie S, "PKSolver: An add-in program for pharmacokinetic and pharmacodynamic data analysis in Microsoft Excel". *Comput Methods Programs Biomed*. **2010**, 99(3), 306-314.
  59. Gao L, Liu G, Ma J, Wang X, Zhou L, Li X, "Drug nanocrystals: in vivo performances". *J Control Release*. **2012**, 160(3), 418-430.
  60. Sigfridsson K, Forssén S, Holländer P, Skantze U, de Verdier J, "A formulation comparison, using a solution and different nanosuspensions of a poorly soluble compound". *Eur J Pharm Biopharm*. **2007**, 67(2), 540-547.
  61. Ponchel G, Montisci M-J, Dembri A, Durrer C, Duchêne D, "Mucoadhesion of colloidal particulate systems in the gastro-intestinal tract". *Eur J Pharm Biopharm*. **1997**, 44(1), 25-31.
  62. Li X, Gu L, Xu Y, Wang Y, "Preparation of fenofibrate nanosuspension and study of its pharmacokinetic behavior in rats". *Drug Dev Ind Pharm*. **2009**, 35(7), 827-833.
  63. Wempe MF, Wright C, Little JL, Lightner JW, Large SE, Caflisch GB, et al., "Inhibiting efflux with novel non-ionic surfactants: Rational design based on vitamin E TPGS". *Int J Pharm*. **2009**, 370(1-2), 93-102.
  64. Abdelwahed W, Degobert G, Stainmesse S, Fessi H, "Freeze-drying of nanoparticles: Formulation, process and storage considerations". *Adv Drug Deliv Rev*. **2006**, 58(15), 1688-1713.
  65. Ramani VD, Jani GK, Sailor GU, "Application of Plackett-Burman Design for Screening of Factors Affecting Pitavastatin Nanoparticle Formulation Development". *Folia Medica (Plovdiv)*. **2020**.
-



Journal of Applied Pharmaceutical Science Vol. 9(10), pp 075-083, October, 2019  
 Available online at <http://www.japsonline.com>  
 DOI: 10.7324/JAPS.2019.91010  
 ISSN 2231-3354



## Development and validation of RP-HPLC method for pitavastatin calcium in bulk and formulation using experimental design

Vinodkumar D. Ramani<sup>1\*</sup>, Girish K. Jani<sup>2</sup>, Ashim Kumar Sen<sup>1</sup>, Girish U. Sailor<sup>3</sup>, Vijaykumar B. Sutariya<sup>4</sup>

<sup>1</sup>Pharmacy Department, Gujarat Technological University, Chandkheda, Ahmedabad 382424, India

<sup>2</sup>K. B. Raval College of Pharmacy, Kasturi Nagar, Gandhinagar 382423, India

<sup>3</sup>Department of Pharmacy, Sumandēp Vidyapeeth, Piparia, Vadodra 391760, India

<sup>4</sup>USF College of Pharmacy, University of South Florida Health, MDC 30, Tampa, FL 33612-4749, USA.

### ARTICLE INFO

Received on: 23/01/2019  
 Accepted on: 02/05/2019  
 Available online: 05/10/2019

#### Key words:

Pitavastatin calcium,  
 RP-HPLC, design of  
 experiment, mobile phase  
 optimization, simplex  
 centroid design.

### ABSTRACT

The optimization of HPLC method involves several variables whose influence has been widely studied. However, in most of the cases, only process variables are taken into account. In this work, the influence of mixture composition on peak quality parameters of Pitavastatin calcium in bulk and tablet dosage form has been studied using a mixture simplex design. A simplex centroid design with axial points in a pseudo-component representation was generated from the pure mixture components. Twelve ternary mixture mobile phases corresponding to augmented design points were tested to separate the drug in sample. The statistical analysis was performed to generate the polynomial equation for each response. The desirability approach was used to determine the optimal mobile phase composition. Furthermore, the method was validated as per the ICH guidelines using specificity, linearity, accuracy, precision, sensitivity, system suitability, and robustness. The results of experimental design were statistically tested for full and in portion to get best fitted model which accurately describe changes in the proportion of these solvents in the mobile phase close to the region of optimal peak quality. The method demonstrated optimum chromatographic separation with isocratic elution of the mobile phase containing a mixture of acetonitrile-water (pH 3.0)-tetrahydrofuran (43:55:02, v/v/v) with a flow rate at 1.0 ml/minute. Design of experiment optimization strategy is a powerful tool to acquire the maximum quality data while performing minimum number of experiments. The mobile phase composition was successfully optimized using simplex centroid mixture design with desirability approach. Additionally, developed method can be applied for routine quantitative analysis of Pitavastatin calcium in bulk and tablet dosage form as it was found to be simple, sensitive, and robust.

### INTRODUCTION

Pitavastatin, chemically (E)-7- [2-cyclopropyl-4-(4-fluorophenyl) quinolin-3-yl]-3,5-dihydroxy- hept-6- enoic acid, is fully synthetic statin and inhibitor of HMG-CoA reductase. Pitavastatin (commonly as a calcium salt) is a more potent antihyperlipidemic agent compared to other statins (Kajinami *et al.*, 2003). The estimation of Pitavastatin calcium (PTV) from pharmaceutical formulations has been conducted using several

analytical methods, including high-performance thin layer chromatography (Akabari *et al.*, 2015; Kumar and Baghyalakshmi 2007; Patel *et al.*, 2011), high performance liquid chromatography (Gomas *et al.*, 2010; Kojima *et al.*, 1999; Panchal *et al.*, 2008), and liquid chromatography-tandem mass spectrometry (Deng *et al.*, 2008; Di *et al.*, 2008). However, there were no reports available in literature to quantify PTV by DoE (design of experiment) approach.

The purpose of optimization strategy is to acquire the maximum quality data while performing a minimum number of experiments. However, in traditional methodology, optimization is carried out by change in one or two parameters deliberately or by trial and error to rule out the relationship among chromatographic parameters. This methodology may become unpredictable and does not take account of possible synergistic effects among variables. Beside this, literature surveys reported the utility of experimental

#### \*Corresponding Author

Vinodkumar D. Ramani, Pharmacy Department, Gujarat Technological University, Chandkheda, Ahmedabad 382424, India.  
 E-mail: vinod.ramani01@gmail.com

© 2019 Vinodkumar D. Ramani *et al.* This is an open access article distributed under the terms of the Creative Commons Attribution 4.0 International License (<https://creativecommons.org/licenses/by/4.0/>).

06/11/2020

06/11/20

06/11/20

06-11-2020

# Development and validation of RP-HPLC method for pitavastatin calcium in bulk and formulation using experimental design

Vinodkumar D. Ramani<sup>1\*</sup>, Girish K. Jani<sup>2</sup>, Ashim Kumar Sen<sup>3</sup>, Girish U. Sailor<sup>3</sup>, Vijaykumar B. Sutariya<sup>4</sup>

<sup>1</sup>Pharmacy Department, Gujarat Technological University, Chandkheda, Ahmedabad 382424, India.

<sup>2</sup>K. B. Raval College of Pharmacy, Kasturi Nagar, Gandhinagar 382423, India.

<sup>3</sup>Department of Pharmacy, Sumandeep Vidyapeeth, Piparia, Vadodara 391760, India.

<sup>4</sup>USF College of Pharmacy, University of South Florida Health, MDC 30, Tampa, FL 33612-4749, USA.

## ARTICLE INFO

Received on: 23/01/2019

Accepted on: 02/05/2019

Available online: 05/10/2019

### Key words:

Pitavastatin calcium, RP-HPLC, design of experiment, mobile phase optimization, simplex centroid design.

## ABSTRACT

The optimization of HPLC method involves several variables whose influence has been widely studied. However, in most of the cases, only process variables are taken into account. In this work, the influence of mixture composition on peak quality parameters of Pitavastatin calcium in bulk and tablet dosage form has been studied using a mixture simplex design. A simplex centroid design with axial points in a pseudo-component representation was generated from the pure mixture components. Twelve ternary mixture mobile phases corresponding to augmented design points were tested to separate the drug in sample. The statistical analysis was performed to generate the polynomial equation for each response. The desirability approach was used to determine the optimal mobile phase composition. Furthermore, the method was validated as per the ICH guidelines using specificity, linearity, accuracy, precision, sensitivity, system suitability, and robustness. The results of experimental design were statistically tested for full and in portion to get best fitted model which accurately describe changes in the proportion of these solvents in the mobile phase close to the region of optimal peak quality. The method demonstrated optimum chromatographic separation with isocratic elution of the mobile phase containing a mixture of acetonitrile-water (pH 3.0)-tetrahydrofuran (43:55:02, v/v/v) with a flow rate at 1.0 ml/minute. Design of experiment optimization strategy is a powerful tool to acquire the maximum quality data while performing minimum number of experiments. The mobile phase composition was successfully optimized using simplex centroid mixture design with desirability approach. Additionally, developed method can be applied for routine quantitative analysis of Pitavastatin calcium in bulk and tablet dosage form as it was found to be simple, sensitive, and robust.

## INTRODUCTION

Pitavastatin, chemically (E)-7- [2-cyclopropyl-4-(4-fluorophenyl) quinolin-3-yl]-3,5-dihydroxy- hept-6- enoic acid, is fully synthetic statin and inhibitor of HMG-CoA reductase. Pitavastatin (commonly as a calcium salt) is a more potent antihyperlipidemic agent compared to other statins (Kajinami *et al.*, 2003). The estimation of Pitavastatin calcium (PTV) from pharmaceutical formulations has been conducted using several

analytical methods, including high-performance thin layer chromatography (Akabari *et al.*, 2015; Kumar and Baghyalakshmi 2007; Patel *et al.*, 2011), high performance liquid chromatography (Gomas *et al.*, 2010; Kojima *et al.*, 1999; Panchal *et al.*, 2008), and liquid chromatography–tandem mass spectrometry (Deng *et al.*, 2008; Di *et al.*, 2008). However, there were no reports available in literature to quantify PTV by DoE (design of experiment) approach.

The purpose of optimization strategy is to acquire the maximum quality data while performing a minimum number of experiments. However, in traditional methodology, optimization is carried out by change in one or two parameters deliberately or by trial and error to rule out the relationship among chromatographic parameters. This methodology may become unpredictable and does not take account of possible synergistic effects among variables. Beside this, literature surveys reported the utility of experimental

\*Corresponding Author

Vinodkumar D. Ramani, Pharmacy Department, Gujarat Technological University, Chandkheda, Ahmedabad 382424, India.

E-mail: [vinod.ramani01@gmail.com](mailto:vinod.ramani01@gmail.com)





Vinodkumar Ramani <vinodramani01@gmail.com>

**[Folia Medica] Manuscript #58174: Accepted**

1 message

Folia Medica <office@foliamedica.bg>

To: vinod.ramani01@gmail.com

Wed, Sep 30, 2020 at 6:27 PM

Cc: pressoffice@pensoft.net, dissemination@pensoft.net, m.kolesnikova@pensoft.net

Dear Vinodkumar Ramani:

We are pleased to inform you that the review process of your manuscript #58174 "Application of Plackett-Burman Design for Screening of Factors Affecting Pitavastatin Nanoparticle Formulation Development" has been completed and it was accepted for publication.

We expect that, even in cases when the revised version is accepted in the form in which it was submitted, there may be some small last-minute changes required or recommended. Please note that reviewers and editors might also have made comments and Track/Change corrections in your manuscript, which you should also check and consider <https://arphahub.com/manual#Handlemanuscriptsunderpeerreview>

We shall expect your final version within 3 days, by 03/10/2020, if not sooner. Additional or supplementary files can also be replaced at this point with corrected versions.

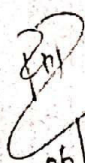
We suggest that you help us increase the visibility of your study and thereby boost its citations and impact by sharing it on social media (i.e. Twitter, Facebook, Mendeley etc.), ideally using both your own and your institution's channels. Information and suggestions on how to promote your work to the international scientific audience and wider public can be found on our website.


Once again, thank you for choosing Folia Medica as the venue for your work!


Folia Medica Editorial office

Pensoft Publishers  
ARPHA Platform

Please do not forward this email as it contains your personal login link.

  
06/11/2020

  
06.11.20

  
06-11-2020



## Article status

My rates  
My manuscripts  
My reviews

My active manuscripts

Filter (14 items found)

Select issue

Manuscript #

ID	Title/Authors	Review type	Status	Action	User	Time remaining
58714	Application of Plackett-Burman design for screening of factors affecting Pitavastatin nanoparticle formulation development	Peer Review	Pending			

## Application of Plackett-Burman design for screening of factors affecting Pitavastatin nanoparticle formulation development

Vinodkumar D. Ramani<sup>1\*</sup>, Girish K. Jani<sup>2</sup>, Girish U. Sailor<sup>3</sup>

<sup>1</sup> Department of Pharmacy, Gujarat Technological University, Ahmedabad, Gujarat, India

<sup>2</sup> Department of Pharmacy, K. B. Raval College of Pharmacy, Gandhinagar, Gujarat, India

<sup>3</sup> Department of Pharmacy, Bhagwan Mahavir College of Pharmacy, Surat, Gujarat, India.

### Corresponding author:

Vinodkumar D. Ramani

Pharmacy Department, Gujarat Technological University, Chandkheda, Ahmedabad-382424, Gujarat, India

Contact details: [vinod.ramani01@gmail.com](mailto:vinod.ramani01@gmail.com)

*[Signature]*  
06/11/2020

*[Signature]*  
06.11.20

*[Signature]*  
06-11-2020